ELSEVIER

Contents lists available at ScienceDirect

Journal of Molecular Spectroscopy

journal homepage: www.elsevier.com/locate/yjmsp





Rotational spectra of twenty-one vibrational states of [³⁵Cl]-and [³⁷Cl]-chlorobenzene

P. Matisha Dorman^a, Brian J. Esselman^a, P. Bryan Changala^b, Michael C. McCarthy^{b,*}, R. Claude Woods^{a,*}, Robert J. McMahon^{a,*}

ARTICLE INFO

Keywords:
Chlorobenzene
Rotational spectroscopy
Microwave
Millimeter-wave
Vibration-rotation interaction
Centrifugal distortion

ABSTRACT

The rotational spectra of [35 Cl]- and [37 Cl]-chlorobenzene (C_6H_5 Cl) have been studied from 2 to 18 GHz and 130–360 GHz, resulting in the measurement, assignment, and least-squares fitting of almost 40,000 transitions of twenty-one vibrational states. Previously measured [35 Cl]- and [37 Cl]-chlorobenzene ground-state transitions were combined with newly measured transitions and fit to A-reduced, partial sextic Hamiltonian models with low-error ($\sigma_{total\ fit}$ <0.05 MHz). Analysis of the 2–18 GHz spectrum allowed for refinement of the nuclear hyperfine coupling constants for the ground-state spectra of both isotopologues, while measurement of the 130–360 GHz spectrum provided sufficient information to determine the sextic centrifugal distortion constants of the ground states for the first time. From these millimeter-wave data collected at room temperature, the spectroscopic constants for the lowest-energy fundamentals of [35 Cl]-chlorobenzene (ν_{20} , ν_{30} , ν_{11} , ν_{14} , ν_{19} , ν_{29} and ν_{18}) and [37 Cl]-chlorobenzene (ν_{20} , ν_{30} , ν_{11}) were determined. As with previous studies of chloroarenes, the computed (B3LYP/6–311+G(2d,p)) spectroscopic constants show quite close agreement with the experimentally determined values.

1. Introduction

Chlorobenzene (C_6H_5Cl , $C_{2\nu}$, $\mu_a = 1.7117$ (14) D [1], $\kappa = -0.85$, Fig. 1) belongs to a family of mono-haloarenes that have been well studied by gas-phase rotational spectroscopy, e.g. fluorobenzene [2,3], chlorobenzene [1,4-7], bromobenzene [1,5], iodobenzene [1,8], polyhalobenzenes [9-11], and haloheteroarenes [12-17]. In addition to their chemical and spectroscopic characteristics as prototypical, simple derivatives of benzene, these species are attractive for investigation due to their large permanent dipole moment created by the highly electronegative halogen substituent and the possibility that they may exist and be detectable in interstellar space. While benzene is a known astrochemical molecule, it cannot be detected by radioastronomy due to its lack of a permanent electric dipole moment. The recent detections of substituted [18-20] and unsubstituted [21,22] aromatic compounds represent dramatic advances in radioastronomy and astrochemistry. Detection of other arenes that are substituted with polar functional groups, such as chlorobenzene, would provide additional tracer molecules that could indicate the presence of aromatic species and provide

insight into their roles in astrochemical reaction networks. Currently, of the approximately 290 molecules that have been detected in the interstellar medium or circumstellar shells, only seven species contain chlorine and only one of those is an organic molecule, chloromethane [23]. The work presented herein expands the measured frequency range for the vibrational ground state of chlorobenzene and, in conjunction with earlier studies [1,4–7], provides a foundation for radioastronomical searches for [35Cl]- and [37Cl]-chlorobenzene in the microwave and millimeter-wave frequency ranges.

The vibrational ground states of [35 Cl]- and [37 Cl]-chlorobenzene have previously been studied by rotational spectroscopy from 8 to 30 GHz and from 150 to 260 GHz [1 ,4–7]. The first microwave study afforded the χ_{aa} nuclear quadrupole coupling constants and rotational constants for both isotopologues, as well as the experimental dipole moment [4]. A subsequent study included additional sets of hyperfineresolved transitions, in which all four $\Delta F = +1$ hyperfine components had been resolved, allowing for the first determination of χ_{aa} , χ_{bb} , and χ_{cc} , as well as the quadrupolar asymmetry parameter (η) [5]. Those hyperfine-resolved transitions were combined with millimeter-wave

E-mail addresses: mmccarthy@cfa.harvard.edu (M.C. McCarthy), rcwoods@wisc.edu (R.C. Woods), robert.mcmahon@wisc.edu (R.J. McMahon).

^a Department of Chemistry, University of Wisconsin-Madison, 1101 University Avenue, Madison, WI 53706-1322, United States

^b Center for Astrophysics, Harvard and Smithsonian, 60 Garden Street, Cambridge, MA 02138-1516, United States

^{*} Corresponding authors.

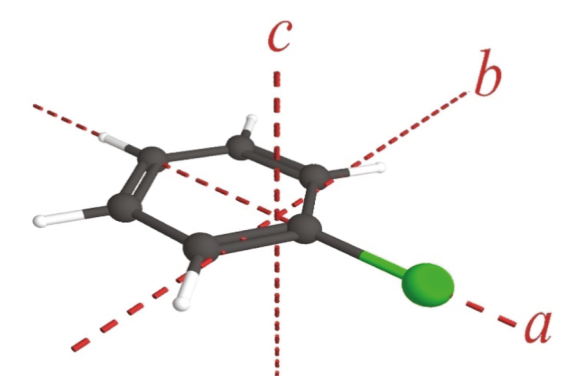


Fig. 1. Chlorobenzene structure ($C_{2\nu}$, $\mu_a=1.71$ D [1]) with principal inertial axes.

data from 150 to 260 GHz to refine the ground-state rotational constants and provide the first determination of the quartic distortion constants [6]. Later, many high-resolution microwave transitions were reported, allowing for refinement of the previously reported spectroscopic constants, calculation of the M_{bb} spin-rotation constant, and improvement in the determination of the electric dipole moment, $\mu_{\alpha} = 1.7117$ (14) D [1].

Although the ground states of [35Cl]- and [37Cl]-chlorobenzene have been well studied [1,4-7], the vibrationally excited states have received less attention. Rotational constants for three vibrationally excited states of chlorobenzene have been reported by high-resolution infrared spectroscopy: ν_5 (A₁, 1483.894 cm⁻¹), ν_{17} (B₁, 741.2240 cm⁻¹), and ν_{10} (A₁, 706.6686 cm⁻¹) [7,24], but pure rotational spectra have not been reported for any of the vibrationally excited states. This circumstance stands in contrast to fluorobenzene [2], bromobenzene [1], and iodobenzene [1], where several low-energy vibrational states for the most abundant isotopologues have been studied by rotational spectroscopy. One additional vibrationally excited state of [35Cl]-chlorobenzene was reported in a synchrotron radiation study, ν_{18} (B₁, 685.59 cm⁻¹), but the data set was insufficient to permit the determination of rotational constants [24]. For v_{10} and v_{17} , a sufficient number of rotationally resolved transitions in the infrared spectrum were assigned, such that a complete set of quartic and a partial set of sextic centrifugal-distortion constants were determined [24]. Low-resolution vibrational [25] and vibronic spectra [26-28] of chlorobenzene have been reported previously; the [³⁵Cl]-chlorobenzene fundamentals below 700 cm⁻¹ are presented in Table 1 and Fig. 2. The reported energies of the fundamentals were used to estimate the combination-state and overtone frequencies displayed in Fig. 2.

The millimeter-wave rotational spectra of the ground and lowenergy vibrationally excited states of several *N*-heterocyclic

Table 1Experimental low-energy fundamental frequencies, symmetries, and calculated transition intensities for chlorobenzene.

	Mode	Symmetry	Experimental Frequency (cm ⁻¹) ^a	Calculated Rotational Transition Intensity at 298 K b
[³⁵ Cl]	ν_{18}	B_1	685.59	0.04
	ν_{29}	B_2	615	0.05
	ν_{19}	B_1	467	0.10
	ν_{14}	A_2	416	0.13
	ν_{11}	A_1	403	0.14
	ν_{30}	B_2	293	0.24
	ν_{20}	B_1	200	0.38
[³⁷ Cl]	ν_{11}	A_1	403	0.05
	ν_{30}	B_2	293	0.07
	ν_{20}	B_1	200	0.13

^a Experimental infrared or Raman fundamental frequencies of chlorobenzene measured from a mixture of natural abundance isotopologues [24–28].

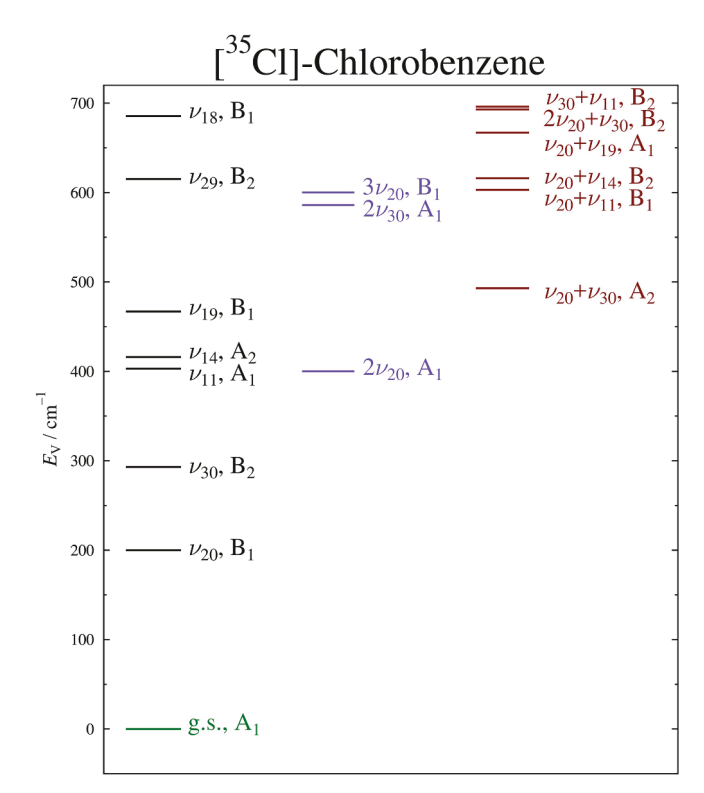


Fig. 2. Vibrational energy levels of [35 Cl]-chlorobenzene below 700 cm $^{-1}$ using experimental vibrational frequencies from [25 -28]. The rotational transitions of $\nu_{30} + \nu_{11}$ were not measured and least-squares fit in this work.

chlorobenzene analogs (2-chloropyrimidine [29], chloropyrazine [16], 2-chloropyridine [17], and 3-chloropyridine [30]) have been studied in the same frequency range as this work (Fig. 3). Spectroscopic constants for over twenty vibrationally excited states were reported for the [35Cl]-and [37Cl]-isotopologues of 2-chloropyridine [17] and chloropyrazine [16], including six fundamentals for the main isotopologue. The current study of chlorobenzene, combined with the earlier work on chloroarenes [16,17,29,30], provides a set of accurate benchmarks for future application of computational methods to predict these spectroscopic constants.

2. Experimental and computational methods

Rotational spectra were collected from a commercial sample of chlorobenzene that was used without additional purification. The

Fig. 3. Chlorobenzene (C_6H_5Cl) and chlorinated *N*-heterocycles studied by rotational spectroscopy: 2-chloropyridine [17], 3-chloropyridine [30], 2-chloropyrimidine [29], and chloropyrazine [16].

^b Relative to [³⁵Cl]-chlorobenzene ground vibrational state.

130 230 GHz and 235 360 GHz spectra were collected on a broadband spectrometer at Wisconsin that has been described previously [31 33]. At room temperature and a pressure of 5 mTorr, rotational spectra were collected at a low flow rate through the sample chamber. The 2 18 GHz spectrum was collected using a chirped-pulse microwave spectrometer at Harvard that has been described previously [34], providing transitions in the vibrational ground state due the supersonic expansion. An experimental frequency uncertainty of 50 kHz was assumed for all new microwave and millimeter-wave measurements, and the reported uncertainties were used for previous works [1,4 6]. Spectral files were combined, visualized, and analyzed using the AABS suite [35,36]. Spectral prediction and least-squares fitting were carried out using Pickett s SPFIT/SPCAT [37] with Kisiel s PIFORM, PISLIN, PMIXC, PLANM, and AC programs for spectroscopic analysis [38,39]. All species in this work were fit to a sextic Hamiltonian in the A- and S-reductions (I^r representation). The data displayed in the manuscript are in the Areduction for direct comparison to previous chloroarene works [1,16,17]. The ground-state spectroscopic constants in both A- and Sreductions are available in the Supplementary Material.

The ability to achieve a low-error fit to a sextic distorted-rotor Hamiltonian enables the determination of highly precise spectroscopic constants for the chloroarenes shown in Fig. 3, which provides a benchmark for the impact of isotopic substitution and vibrational excitation on the spectroscopic constants. It has become a standard practice to predict the rotational and centrifugal distortion constants, through the sextic constants, for the ground states of different isotopologues, using anharmonic frequency calculations [11,31,32,40 43]. In contrast, with a few exceptions [44 48], prediction of the centrifugal distortion constants of vibrationally excited states has remains a largely unsolved problem for the spectroscopic community. While it is possible via a number of computational software packages to predict the vibration rotation interaction constants for the fundamental vibrational modes, no commonly implemented method is available for predicting the centrifugal distortion constants of the vibrationally excited states encountered in this work. Accurate prediction of the vibration rotation interaction constants greatly facilitates the initial prediction of spectra and assignment of the vibrationally excited states for the chloroarenes. In the previous works [16,17], transitions for a substantial number of vibrationally excited states through four-quanta vibrations can be leastsquares fit to single-state Hamiltonians from 130 to 360 GHz. This result is remarkable, given the presence of over a dozen vibrationally excited states below 700 cm ¹ for each of these molecules. Even for states quite close in energy, where attempts were unsuccessful in treating them as Coriolis-coupled dyads, e.g. 26 and 18 of 2-chloropyridine [17], all of the vibrationally excited-state spectroscopic constants determined in the analysis appear to be largely free of the effects of untreated Coriolis

The molecular geometries of [35Cl]- and [37Cl]-chlorobenzene were optimized, and anharmonic frequency calculations were performed using density functional theory calculations (B3LYP/6 311 G(2d,p)) as implemented in Gaussian 16 [49] with the WebMO interface [50]. Calculations utilized very tight convergence criteria (opt verytight and int grid ultrafine) and afforded predicted values of the anharmonic vibrational frequencies, vibration rotation interaction constants B_e), and ground-state quartic and sextic centrifugal distortion constants. Combined with the experimental ground-state spectroscopic constants, the calculated vibration rotation interaction constants provided the initial predictions of the spectroscopic constants for the vibrationally excited-state species. In cases where we were unable to satisfactorily determine a ground-state spectroscopic constant, the value was held fixed at the corresponding computed value (B3LYP/6 311 G (2d,p)). When the value of a spectroscopic constant for a fundamental vibration could not be satisfactorily determined, it was held constant at the corresponding ground-state value. In a similar manner to the other chloroarene studies [16,17], the constants that could not be satisfactorily determined for overtone and combination states were held constant at values extrapolated from lower-energy vibrational states. Additionally, predicted nuclear quadrupole coupling ($_{aa}$, $_{bb}$, and $_{cc}$) and nuclear spin-rotation (M_{aa} , M_{bb} , and M_{cc}) constants were calculated at the optimized geometry. Computational output files are provided in the Supplementary Material.

3. Spectral and computational analysis

The rotational spectrum of chlorobenzene (Fig. 4) is dominated by atype, R-branch transitions that resemble the typical band structure of monosubstituted aromatic molecules [3,16,17,33,51 53]. Typical of a chloroarene [16,17], the spectrum of chlorobenzene is highly congested with transitions from the [35Cl]- and [35Cl]-isotopologues in their ground and vibrationally excited states. Chlorobenzene displays an oblate-type band structure, in which the lead transition in each obvious band is comprised of two degenerate transitions with $K_a = 0$ and 1 and equal values of K_c . As the transitions in the band progress to decreasing values of J and K_c and increasing values of K_a , the transitions sharing the same value of K_c lose degeneracy and eventually become degenerate with transitions sharing the same value of K_a . The nuclear quadrupole moment of the chlorine nucleus creates well-resolved hyperfine transitions at low frequency and partially-resolved hyperfine transitions from 130 to 360 GHz. Weaker Q-branch transitions were obscured by the transitions of many vibrational states that appear in the room temperature 130 360 GHz spectrum and were only observable in the cold sample (FTMW spectrum; 18 GHz) that did not contain transitions from the vibrationally excited states. No P-branch transitions were observed in any spectral range for chlorobenzene. The spectra of all four [¹³C]-chlorobenzene isotopologues were sufficiently intense, relative to the spectra of vibrationally excited states, that they could be assigned at natural abundance. The detailed analysis of the rotational spectra of [¹³C]- and [²H]-containing isotopologues will be the subject of a future publication, whose objective is the determination of a highly precise and accurate semi-experimental (r_e^{SE}) structure of chlorobenzene.

3.1. [35Cl]-Chlorobenzene, vibrational ground state

Over 5500 hyperfine-resolved and unresolved transitions were newly measured for the ground state of chlorobenzene (2 18 GHz and 130 360 GHz); these data were combined with all previously reported measurements [1,4 6]. Where transitions were re-measured from previous works, the value in closest agreement with the least-squares fit was included in the final data set. A cumulative total of 6039 independent transitions from 2 to 360 GHz were measured, assigned, and leastsquares fit to a sextic distorted-rotor Hamiltonian that also addressed chlorine nuclear quadrupole coupling and nuclear spin-rotation coupling. Hyperfine-resolved transitions were measured between 2 and 18 GHz, while partially resolved hyperfine frequencies, for which the quartet of transitions (F J $\frac{1}{2}$ J $\frac{1}{2}$ J $\frac{3}{2}$ J $\frac{3}{2}$) have collapsed into doublets (F J $\frac{1}{2}$ J $\frac{3}{2}$), were measured between 130 and 360 GHz. In the latter frequency range, these partially resolved doublets were common for transitions with K_a 20 and J 90. Previously, Dorosh et al. [1] noted that the inclusion of the nuclear spinrotation constant (M_{bb}) in the Hamiltonian reduced the deviations of the transitions in the least-squares fit, and a similar approach was taken in the current study. A data distribution plot with transition quantum numbers up to K_a 70 and J 145 is provided in Fig. 5, which includes all previous measurements. Computed and experimental spectroscopic constants (A-reduced Hamiltonian, I^r representation) of [³⁵Cl]-chlorobenzene are provided in Table 2.

Both the experimental spectroscopic constants of a previous work [1] and the B3LYP-computed values are in quite good agreement with the newly determined ground-state values presented in Table 2. As expected, the addition of several thousand transitions reduces the statistical uncertainty in each constant. The values of A_0 , B_0 , and C_0

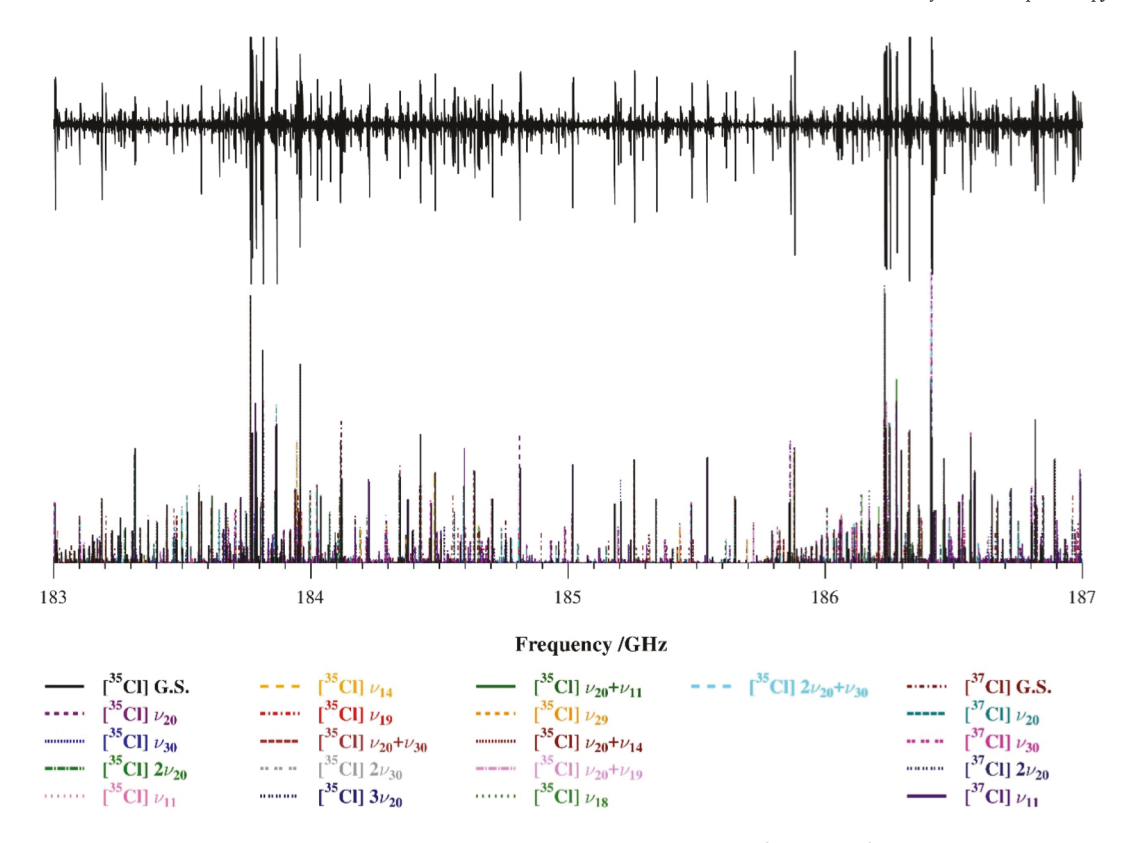


Fig. 4. Rotational spectrum of chlorobenzene from 183 to 187 GHz with predicted stick spectra for [35Cl]- and [37Cl]-chlorobenzene ground and vibrationally excited states.

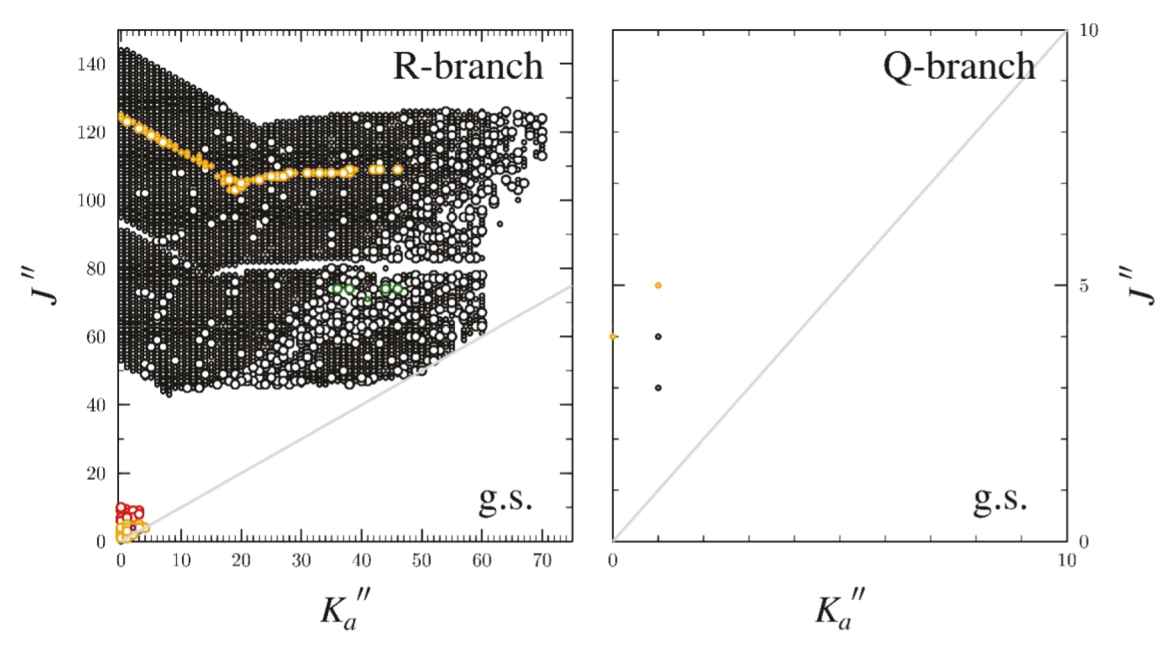


Fig. 5. Data distribution plots for the least-squares fit of spectroscopic data for the ground state of [35 Cl]-chlorobenzene from the current work (black circles) and the measurements from Dorosh *et al.* (orange) [1], Kisiel (green) [6], Caminati and Mirri (purple) [5], and Poynter (red) [4]. The size of the outlined circles in this plot corresponds to $|(f_{obs.} - f_{calc.})/\delta f|$, where δf is the measurement uncertainty. Data distribution plots for other states are available in the Supplementary Material. (For interpretation of the references to colour in this figure legend, the reader is referred to the web version of this article.)

determined previously and in this work are in complete agreement within the estimated statistical uncertainties of each value. The agreement is not quite as good for the quartic centrifugal distortion constants, where none of the values agree within their statistical uncertainties. This is likely due to the smaller set of previously available transition

frequencies preventing the inclusion of sextic centrifugal distortion constants. The B3LYP-computed rotational constants are in excellent agreement with the experimental values, especially for the A_0 constant (0.004%, 1.3%, and 1.0% error for A_0 , B_0 , and C_0 , respectively). The quartic distortion constants are within 3.2% of the experimental values,

 Table 2

 Spectroscopic constants for $[^{35}Cl]$ -chlorobenzene in its ground and vibrationally excited states (A-reduced Hamiltonian, I^r representation).

	B3LYP ^a	[³⁵ Cl] G.S. [1]	[³⁵ Cl] G.S. ^b	20	30
				B ₁ , 200 cm ^{1 c}	B ₂ , 293 cm ^{1 c}
$A_{\nu}^{(A)}$ (MHz)	5672.	5672.27684 (21)	5672.27687 (16)	5640.4702 (10)	5701.9631 (14)
$B_{\nu}^{(A)}$ (MHz)	1556.	1576.786654 (29)	1576.786667 (18)	1577.893269 (45)	1576.871980 (51)
$C_{\nu}^{(A)}$ (MHz)	1221.	1233.675003 (28)	1233.675023 (18)	1235.053633 (42)	1232.815361 (46)
-, ()			(,		(11)
(l-Ha)	0.060	0.0602076 (25)	0.0603301 (19)	0.0600200 (26)	0.0604022 (22
J (kHz)		0.0602876 (25)		0.0608399 (26)	0.0604032 (33
_{JK} (kHz)	0.286	0.281797 (32)	0.281682 (12)	0.288343 (17)	0.273588 (24)
_K (kHz)	0.839	0.8694 (34)	0.87107 (99)	0.5581 (10)	1.1793 (19)
_J (kHz)	0.0142	0.01446596 (95)	0.01448584 (98)	0.0145607 (18)	0.0145172 (20
_K (kHz)	0.305	0.30693 (16)	0.307516 (89)	0.29048 (11)	0.32665 (13)
(0.00100		0.000500 (05)	0.00005 (10)	0.00004 (1.4)
_J (mHz)	0.00183		0.002529 (85)	0.00295 (10)	0.00284 (14)
_{JK} (mHz)	0.112		0.1061 (53)	0.10804 (72)	0.1587 (78)
_{KJ} (mHz)	0.542		0.524 (19)	0.2534 (57)	1.013 (28)
_K (mHz)	0.976		[0.976] ^e	[0.976] ^f	[0.976] ^f
$_{J}$ (mHz)	0.00115		0.001372 (42)	0.001392 (60)	0.001520 (71
_{JK} (mHz)	0.0623		0.0654 (36)	0.0927 (41)	0.0554 (57)
_K (mHz)	1.54		1.516 (92)	$[1.52]^f$	2.45 (14)
(MII-)	60.0	71 2250 (12)	71 2250 (11)	72.02.(17)	79.66 (99)
aa (MHz)	68.2	71.2359 (13)	71.2359 (11)	73.93 (17)	73.66 (23)
bb (MHz)	37.5	38.2153 (15)	38.21533 (57)	[39.56] ⁿ	[39.43] ⁿ
cc (MHz)	30.7	33.0205 (15)	33.0205 (16)	[34.36] ⁿ	[34.23] ⁿ
-	0.1006	0.072924 (30)	0.072924 (11)	0.0729 (16)	0.0705 (22)
M _{aa} (kHz) ^j	0.483	. === (0.0)	. =	5 0 mag f	5 0 mag f
M_{bb} M_{cc})/2 (kHz) ^j	0.527	0.525 (83)	0.520 (65)	[0.520] ^f	[0.520] ^f
$I_{ m lines}^{\ \ k}$		424	6039	4446	3673
total fit (MHz)		121	0.029	0.026	0.030
total fit (IVIIIE)		0.701	0.564	0.571	0.602
w.fit l i (uÅ ²) m		0.044977 (11)	0.044959 (7)	0.689930 (23)	0.811836 (29)
	2 20	11	14	19	20 30
	A ₁ , 400 cm ¹	A ₁ , 403 cm ^{1 c}	A ₂ , 416 cm ^{1 c}	B ₁ , 467 cm ^{1 c}	A ₂ , 493 cm ¹
(A) (2 577)					
$A_{\nu}^{(A)}$ (MHz)	5611.04379 (97)	5669.9515 (17)	5667.1189 (17)	5671.136 (23)	5669.7845 (30)
B _ν ^(A) (MHz)	1578.962778 (36)	1575.993672 (67)	1577.039126 (73)	1576.6042 (23)	1577.96305 (23)
$C_{\nu}^{(A)}$ (MHz)	1236.386027 (30)	1233.257669 (58)	1234.380172 (59)	1234.259058 (93)	1234.206200 (80
$_{J}$ (kHz)	0.06145692 (95)	0.0605564 (45)	0.0604736 (44)	0.06041 (16)	0.061013 (2
_{JK} (kHz)	0.288693 (36)	0.285333 (48)	0.281605 (40)	0.2928 (65)	0.2768 (22)
	0.3722 (11)	0.7301 (22)	0.8819 (20)	[0.87107] ^f	0.716 (29)
(kHz)	0.01462971 (55)			0.014480 (83)	0.014666 (1
_J (kHz)	, ,	0.0145694 (26)	0.0145032 (28)		
_K (kHz)	0.275267 (89)	0.30513 (18)	0.30800 (17)	0.3111 (13)	0.3084 (12)
_J (mHz)	[0.00337]	0.00326 (19)	0.00269 (18)	0.00242 (22)	0.00226 (15
JK (mHz)	0.1021 (16)	0.1723 (81)	0.0902 (51)	0.247 (21)	[0.161] ^h
	[0.] ^g	[0.524] ^f	[0.524] ^f		[0.742] ^h
(mHz)	[0.976] ^f	[0.976] ^f	[0.976] ^f	[0.524] ^f [0.976] ^f	[0.976] ^f
(mHz)	[0.976] ⁵ [0.001412] ^h	0.001408 (94)	0.001429 (97)	[0.976] ⁷	[0.00154] h
J (mHz)		, ,			
_{JK} (mHz)	0.1254 (32)	0.0869 (72)	0.0645 (66)	[0.0654] ^f	[0.0827] h
_K (mHz)	[1.52] ^h	2.69 (15)	1.17 (10)	[1.52] ^f	[2.45] ^h
$J_{ m lines}^{k}$	2953	2696	2724	597	586
total fit (MHz)	0.033	0.036	0.036	0.037	0.040
w.fit	0.654	0.711	0.723	0.746	0.795
w.fit	1.383844 (20)	0.014206 (36)	0.218826 (36)	0.20389 (59)	0.068446 (7
$_{i}$ (uÅ ²) m	<u> </u>		20 11	29	20 14
_i (uÅ ²) ^m	2 30	3 20			
_i (uÅ ²) ^m		3 ₂₀ B ₁ , 600 cm ¹		B ₂ , 615 cm ^{1 c}	B ₂ , 616 cm ¹
	A ₁ , 586 cm ¹	B ₁ , 600 cm ¹	B ₁ , 603 cm ¹	B ₂ , 615 cm ^{1 c} 5665,2743 (99)	B ₂ , 616 cm ¹ 5636.216 (52)
	A ₁ , 586 cm ¹ 5731.484 (34)	B ₁ , 600 cm ¹ 5583.216 (14)	B ₁ , 603 cm ¹ 5634.550 (13)	5665.2743 (99)	5636.216 (52)
λ _ν ^(A) (MHz) β _ν ^(A) (MHz)	A ₁ , 586 cm ¹	B ₁ , 600 cm ¹	B ₁ , 603 cm ¹		5636.216 (52) 1578.1150 (47)
λ _ν ^(A) (MHz) β _ν ^(A) (MHz)	A ₁ , 586 cm ¹ 5731.484 (34) 1576.9857 (31)	B ₁ , 600 cm ¹ 5583.216 (14) 1580.0151 (13)	B ₁ , 603 cm ¹ 5634.550 (13) 1577.1510 (12)	5665.2743 (99) 1576.8511 (10)	5636.216 (52) 1578.1150 (47)
$A_{\nu}^{(A)}$ (MHz) $B_{\nu}^{(A)}$ (MHz)	A ₁ , 586 cm ¹ 5731.484 (34) 1576.9857 (31)	B ₁ , 600 cm ¹ 5583.216 (14) 1580.0151 (13)	B ₁ , 603 cm ¹ 5634.550 (13) 1577.1510 (12) 1234.713201 (97) 0.060503 (21)	5665.2743 (99) 1576.8511 (10)	5636.216 (52) 1578.1150 (47) 1235.735599 (9 0.06038 (47
$\Lambda_{\nu}^{(\Lambda)}$ (MHz) $\lambda_{\nu}^{(\Lambda)}$ (MHz) $\Gamma_{\nu}^{(\Lambda)}$ (MHz)	A ₁ , 586 cm ¹ 5731.484 (34) 1576.9857 (31) 1231.941258 (82)	B ₁ , 600 cm ¹ 5583.216 (14) 1580.0151 (13) 1237.693066 (38)	B ₁ , 603 cm ¹ 5634.550 (13) 1577.1510 (12) 1234.713201 (97)	5665.2743 (99) 1576.8511 (10) 1232.817625 (88)	5636.216 (52) 1578.1150 (47) 1235.735599 (9
$A_{\nu}^{(A)}$ (MHz) $3_{\nu}^{(A)}$ (MHz) $C_{\nu}^{(A)}$ (MHz) J (kHz)	A ₁ , 586 cm ¹ 5731.484 (34) 1576.9857 (31) 1231.941258 (82) 0.05898 (26)	B ₁ , 600 cm ¹ 5583.216 (14) 1580.0151 (13) 1237.693066 (38) 0.062260 (54)	B ₁ , 603 cm ¹ 5634.550 (13) 1577.1510 (12) 1234.713201 (97) 0.060503 (21)	5665.2743 (99) 1576.8511 (10) 1232.817625 (88) 0.063492 (86)	5636.216 (52) 1578.1150 (47) 1235.735599 (9 0.06038 (47
$A_{\nu}^{(A)}$ (MHz) $3_{\nu}^{(A)}$ (MHz) $C_{\nu}^{(A)}$ (MHz) $J_{\nu}^{(A)}$ (MHz) $J_{\nu}^{(A)}$ (kHz) $J_{\nu}^{(A)}$ (kHz) $J_{\nu}^{(A)}$ (kHz)	A ₁ , 586 cm ¹ 5731.484 (34) 1576.9857 (31) 1231.941258 (82) 0.05898 (26) 0.308 (11)	B ₁ , 600 cm ¹ 5583.216 (14) 1580.0151 (13) 1237.693066 (38) 0.062260 (54) 0.3011 (23)	B ₁ , 603 cm ¹ 5634.550 (13) 1577.1510 (12) 1234.713201 (97) 0.060503 (21) [0.2910] ^h	5665.2743 (99) 1576.8511 (10) 1232.817625 (88) 0.063492 (86) 0.1612 (36)	5636.216 (52) 1578.1150 (47) 1235.735599 (9 0.06038 (47 0.332 (19)
$A_{\nu}^{(A)}$ (MHz) $B_{\nu}^{(A)}$ (MHz) $C_{\nu}^{(A)}$ (MHz) $B_{\nu}^{(A)}$ (MHz) $B_{\nu}^{(A)}$ (MHz)	A ₁ , 586 cm ¹ 5731.484 (34) 1576.9857 (31) 1231.941258 (82) 0.05898 (26) 0.308 (11) [1.488] ^h	B ₁ , 600 cm ¹ 5583.216 (14) 1580.0151 (13) 1237.693066 (38) 0.062260 (54) 0.3011 (23) [0.] ^g	B ₁ , 603 cm ¹ 5634.550 (13) 1577.1510 (12) 1234.713201 (97) 0.060503 (21) [0.2910] ^h [0.4171] ^h	5665.2743 (99) 1576.8511 (10) 1232.817625 (88) 0.063492 (86) 0.1612 (36) [0.87107] ^f	5636.216 (52) 1578.1150 (47) 1235.735599 (9 0.06038 (47 0.332 (19) [0.5689] ^h

Table 2 (continued)

, ,					
, (mHz)	0.00456 (21)	[0.00379] ^h	0.00268 (19)	0.00393 (21)	[0.00311] h
_{JK} (mHz)	[0.211] h	[0.112] h	[0.174] ^h	$[0.1061]^f$	[0.0921] h
_{KJ} (mHz)	[1.50] ^h	[0.1 ^g	[0.253] ^h	[0.524] ^f	[0.253] ^h
_K (mHz)	[0.976] ^f	[0.976] ^f	[0.976] ^f	[0.976] ^f	[0.976] ^f
, (mHz)	[0.00167] ^h	[0.00143] ^h	[0.00143] ^h	[0.001372] ^f	[0.00145] h
_{JK} (mHz)	[0.0454] ^h	[0.147] ^h	[0.114] ^h	[0.0654] ^f	[0.0918] h
_K (mHz)	[3.38] ^h	$[1.52]^{h}$	[2.69] ^h	[1.52] ^f	$[1.17]^{h}$
$N_{ m lines}^{\ \ k}$	545	819	434	491	471
total fit (MHz)	0.040	0.034	0.042	0.042	0.043
w.fit	0.813	0.680	0.845	0.858	0.856
$i \left(u \mathring{A}^2 \right)^m$	1.58233 (82)	2.05125 (35)	0.82199 (32)	0.23285 (39)	0.9383 (13)
	20	19	18	<u>` ` ` ` </u>	2 20 30
	A ₁ .	667 cm ¹	B ₁ , 685.59 cn	n ^{1 d}	B ₂ , 693 cm ¹
$A_{v}^{(A)}$ (MHz)					
$B_{\nu}^{(A)}$ (MHz)		39.2712 (91)	5674.79 (22)		5641.1 (11) 1578.942 (88)
$C_{\nu}^{(A)}$ (MHz)		77.72274 (96) 35.619398 (78)	1575.624 (19 1232.68845 (1235.54782 (42)
G _y . (MHZ)	123	55.019596 (76)	1232.06643 (.30)	1233.34762 (42)
, (kHz)		0.06135 (12)	0.05234 ((60)	0.06244 (73)
J (kHz)		0.2865 (48)	[0.281682		[0.2869] h
K (kHz)		[0.5581] h	[0.87107]		[0.5534] h
, (kHz)		0.014784 (59)	0.01083 (0.01530 (36)
_K (kHz)		0.2925 (11)	0.5581 (9	• •	0.314 (13)
K ()				-,	*****
J (Hz)		[0.00284] ^h	[0.002529	1 f	[0.00368]
_{JK} (Hz)		0.301 (19)	[0.10611 ^f		[0.163] h
_{KJ} (Hz)		0.253] ^h	[0.524] ^f		[0.472] ^h
κ (Hz)		[0.976] ^f	[0.976] ^f		[0.976] ^f
_J (Hz)		[0.00139] ^h	[0.001372	1^f	[0.00156] h
_{JK} (Hz)		[0.0927] ^h	[0.0654] ^f	-	$[0.110]^{h}$
K (Hz)		[1.516] ^h	[1.516] ^f		[2.45] ^h
K (212)			[1.010]		[2. 10]
$N_{ m lines}^{k}$	36	58	90		76
total fit (MHz)		0.044	0.051		0.043
w fit		0.872	1.024		0.857
$i^{\text{w.iii}}$ (uÅ ²) m		0.93096 (24)	0.1758 (5	(2)	0.631 (25)

^a Evaluated with the 6 311 G(2d,p) basis set. ^b This work. Includes transitions from previous works [1,4 6], ^c Vibrational frequencies from [25 28]. ^d High-resolution vibrational frequencies from [24]. ^e Value held constant at its B3LYP/6 311 G(2d,p) value. ^f Value held constant at its ground state value. ^g Value held constant at zero because extrapolated value changed sign relative to corresponding values in lower-energy states. ^h Value held constant at the value extrapolated from lower-energy states in corresponding series. Extrapolation based upon an appropriate polynomial (for overtone states) or a linear combination of values (for combination states). ^l Nuclear quadrupole asymmetry parameter, bb cc aa ^j Nuclear spin-rotation constants consistent with sign convention H_{sr} IMJ. ^k Number of assigned transition frequencies. ^l Weighted error of least-squares fit. ^m Inertial defect (i I_c I_a I_b). ⁿ The difference between bb and cc was held constant at the ground-state value. The values of bb and cc were calculated using the assumption that a bb cc 0.

with the largest error in $_K$. All sextic distortion constants were able to be satisfactorily determined for the first time, except for $_K$ which was held constant at the B3LYP value. The inability to obtain a complete set of sextic centrifugal distortion constants is consistent with the previous work on 2-chloropyridine [17] and chloropyrazine [16], indicating that this problem is likely due to the fact that the measured frequency range (up to 360 GHz) does not afford sufficient data for a molecule of this composition with only a-type transitions. The remaining sextic distortion constants are accurately predicted within 21% of the experimental values, suggesting that the experimental values are physically meaningful.

The previously reported values of the nuclear quadrupole coupling constants [1] display good agreement with the refined experimental values from the current study. Inclusion of many new hyperfine-resolved and unresolved transitions in this work changes the values and uncertainties in aa, bb, and cc only slightly, suggesting the previously reported range of data provides sufficient information for the least-squares fit to completely determine those constants for the ground state. The B3LYP-computed values accurately predict the coupling constants within 4.2%, 1.8%, and 7.1% of the aa, bb, and cc experimental values. Since the coupling constants did not change significantly

in the current analysis, the nuclear quadrupole asymmetry parameter () is nearly identical to the reported value, with a slight decrease in the uncertainty. Following the method of Dorosh $et\,al.$ [1], the nuclear spin-rotation constants were also experimentally determined in this work. The value of $(M_{bb} \ M_{cc})/2$ is in excellent agreement with the previously reported value. The predicted value of $(M_{bb} \ M_{cc})/2$ is within 1.3% of the experimentally determined value, so we attempted to include the predicted value of M_{aa} in the least-squares fit. Doing so did not reduce the overall value of the fit, so we elected to exclude this constant from the fit to remain consistent with the previous work [1].

The first excited vibrational state of chlorobenzene, $_{20}$, is the out-of-plane bending motion of the chlorine atom with respect to the benzene ring (B₁, 200 cm $^{-1}$). The fundamental was identified in the 130 360 GHz region using the ground-state spectroscopic constants modified with the B3LYP-predicted vibration rotation interaction constants to predict A_{20} , B_{20} , and C_{20} . Like the ground state, K_a series 20 with low values of J appear as hyperfine doublets that were included in the least-squares fit. Calculated to be 38% of the ground-state intensity and with

no microwave transitions available, we were only able to determine $_{aa}$ and held the remaining nuclear coupling term ($_{bb}$ $_{cc}$)/4 constant at the experimental ground-state value. Over 4400 independent frequency transitions were included for $_{20}$ with K_a series from 0 to 55. The experimental vibration rotation interaction constants are well predicted by the B3LYP calculation, and the largest error is in A_0 A_{20} (obs. calc.

0.73 MHz (2.3%)). A comparison of the B3LYP-predicted and experimental vibration rotation interaction constants for all observed vibrational states in this work is presented in Table 3. For the quartic and sextic centrifugal distortion constants, the uncertainties, signs, and order-of-magnitude are comparable to the analogous ground-state constants, suggesting the excited-state values are physically meaningful. The distortion constants are reasonably well determined except for $_K$ and $_K$, which needed to be held constant at their ground-state values. Data distribution plots and the least-squares fitting files of all collected frequencies can be seen in the Supplementary Material for $_{20}$ and all other excited vibrational state of chlorobenzene.

The K_a 0 series of both 2 $_{20}$ (A₁, 400 cm $^{-1}$) and 3 $_{20}$ (B₁, 600 cm $^{-1}$) were well predicted using the extrapolated values of the 20 ground-state vibrational series. Fig. 6 depicts the relative spectroscopic constants of the 20 series as a function of vibrational excitation. Since both vibrational states are only 3 cm 1 away from their closest vibrational neighbors ($_{11}$ A₁, 403 cm 1 and $_{20}$ $_{11}$ B₁, 603 cm 1), frequency perturbations were expected in the rotational spectra. As a result, their spectroscopic parameters must be analyzed carefully to ensure that they are physically meaningful and that they have not been impacted by unaddressed coupling. Indeed, in a Loomis-Wood plot of both vibrational states at high K_a , series obviously contain perturbation and gradually deviate as a function of J from distorted-rotor frequencies without ever returning to the predicted values in our frequency range. No large local resonances were observed in their spectra and, as a result, a least-squares fit of these species using a Coriolis-coupled dyad was not attempted. Hyperfine doublets were observed for 2 20 at similar values of K_a and J as that of 20. At 14% of the ground-state intensity, however,

Table 3 Vibration-rotation interaction constants of chlorobenzene (A-reduced Hamiltonian, I^{Γ} representation).

		[³⁵ Cl]-chlorobenzer	ne	[³⁷ Cl]-chlorobenzer	ne
		Experimental	B3LYP ^a	Experimental	B3LYP ^a
		20		20	
A_0	A_{20} (MHz)	31.8067 (10)	32.5	32.0605 (17)	32.7
B_0	B_{20} (MHz)	1.106602 (49)	1.08	1.088761 (66)	1.06
C_0	C_{20} (MHz)	1.378610 (46)	1.34	1.348343 (61)	1.32
		30		30	
A_0	A_{30} (MHz)	29.6862 (14)	30.3	29.9315 (22)	30.5
B_0	B_{30} (MHz)	0.085313 (54)	0.08	0.079887 (81)	0.08
C_0	C_{30} (MHz)	0.859662 (49)	0.90	0.840843 (68)	0.88
		11		11	
A_0	A_{11} (MHz)	2.3254 (17)	0.09	2.665 (71)	0.12
B_0	B_{11} (MHz)	0.792995 (69)	1.04	0.7888 (56)	1.03
C_0	C_{11} (MHz)	0.417354 (61)	0.55	0.39384 (11)	0.54
		14			
A_0	A_{14} (MHz)	5.1580 (17)	5.3		
B_0	B_{14} (MHz)	0.252459 (75)	0.23		
C_0	C_{14} (MHz)	0.705149 (62)	0.68		
		19			
A_0	A_{19} (MHz)	1.141 (23)	1.6		
B_0	B_{19} (MHz)	0.1825 (23)	0.22		
C_0	C_{19} (MHz)	0.584035 (95)	0.55		
		29			
A_0	A_{29} (MHz)	7.003 (10)	5.9		
B_0	B_{29} (MHz)	0.0644 (10)	0.10		
C_0	C_{29} (MHz)	0.857398 (90)	1.01		
		18			
A_0	A_{18} (MHz)	2.51 (22)	4.5		
B_0	B_{18} (MHz)	1.163 (19)	0.33		
C_0	C_{18} (MHz)	0.98657 (30)	0.13		

^a Evaluated with the 6 311 G(2d,p) basis set.

they were not able to be included in the 2 $_{20}$ fit or any fit for vibrational states $_{400}$ cm $_{1}$. Despite these limitations, almost 3000 total transitions were included for 2 $_{20}$ and over 800 for 3 $_{20}$. For 2 $_{20}$, only $_{JK}$, and $_{JK}$ were allowed to vary in the least-squares fit. Least-squares fitting of the remaining sextic centrifugal distortion constants either did not converge or converged to values far from the v $_{20}$ parameter-series extrapolations (similar to the extrapolations shown in Fig. 6). In the latter cases, those centrifugal distortion constants were held constant at their linearly extrapolated values. For 3 $_{20}$, $_{K}$ and $_{KJ}$ were held constant at a value of zero, because their extrapolated value passed through zero and their values could not be determined in the least-squares fitting. All of the remaining sextic centrifugal distortion constants were held at values extrapolated from the respective v $_{20}$ parameter series using a linear or quadratic model as appropriate.

In Fig. 6, the relative spectroscopic constants of the 20 series are plotted versus vibrational excitation. All non-zero values are plotted and all points in the series were modeled by an appropriate-order polynomial. All of the relative spectroscopic constants and the inertial defects exhibit nearly linear changes as a function of vibrational quantum. Similar to previously studied chloroarenes, the purely K-dependent quartic distortion constants show larger changes than purely J-dependent terms [16,17]. Due to their reduced intensity, fewer transitions could be included for subsequent, high-energy members of the vibrational series, and more constants were required to be held constant at their extrapolated values. Holding undeterminable constants to the extrapolated estimates typically results in a lower total fit uncertainty, in contrast to holding the value of the constant at its corresponding fundamental value or zero. If the estimated value changes sign compared to the same constant in the other vibrational quanta, however, the value is instead held constant at zero (usually resulting in a lower $_{\rm total\; fit}$). For the $_{20}$ series, the relative values of the $J\text{-}{\rm dependent}$ quartic centrifugal distortion constants ($_J$ and $_J$) display smooth changes with increasing vibrational excitation through 3 20. The change in $_{\it JK}$ is non-monotonic and it appears that the value of $_{\it JK}$ for 2 $_{\it 20}$ is too small. This appears to be linked to the behavior of K, which may be slightly too large. The behavior of K is ambiguous as this constant has been known to display greater curvature upon vibrational excitation than the other quartic centrifugal distortion constants (e.g., v 24 of diketene [54]). Of the few sextic centrifugal distortion constants that are able to be varied for 2 $_{20}$, $_{JK}$ and $_{JK}$ are close to their respective linearly extrapolated values (Fig. 6). As a result of both 2 20 and 3 20 being only 3 cm⁻¹ away from other vibrationally excited states, the quartic and sextic centrifugal distortion constants that are allowed to vary in the fit are likely absorbing some untreated perturbation as a result of state mixing with their near-energy neighboring states. To minimize the impact of these perturbations, we included only the most intense unperturbed spectral transitions but excluded some transitions that, although assignable, had an adverse impact on the least-squares fit.

3.3. [35 Cl]-Chlorobenzene, $_{30}$ (v 1, 2)

The second lowest-energy fundamental of [35 Cl]-chlorobenzene, $_{30}$ (B₂, 312 cm 1), is an in-plane bending vibration of the chlorine atom with respect to the benzene ring. The B3LYP-computed vibration rotation interaction terms provided excellent starting predictions of the rotational constants, with the largest magnitude discrepancy proving to be in the A_0 A_{30} constant (*obs. calc.* 0.60 MHz, 2.0%). A total of 3673 transitions were included in the final distorted-rotor fit, with all constants well determined except for $_{K}$. The quartic and sextic distortion terms agree, both in sign and order of magnitude, with the ground-state constants, suggesting they are reasonably determined and physically meaningful. Like $_{20}$, K_a series 20 displayed hyperfineresolved doublets that were sufficiently intense to include in the least-squares fit. Only the $_{aa}$ coupling constant was able to be determined and was found to be of similar magnitude to that in $_{20}$. The second overtone, 3 $_{30}$ (A₁, 585 cm 1), was easily predicted using a linear

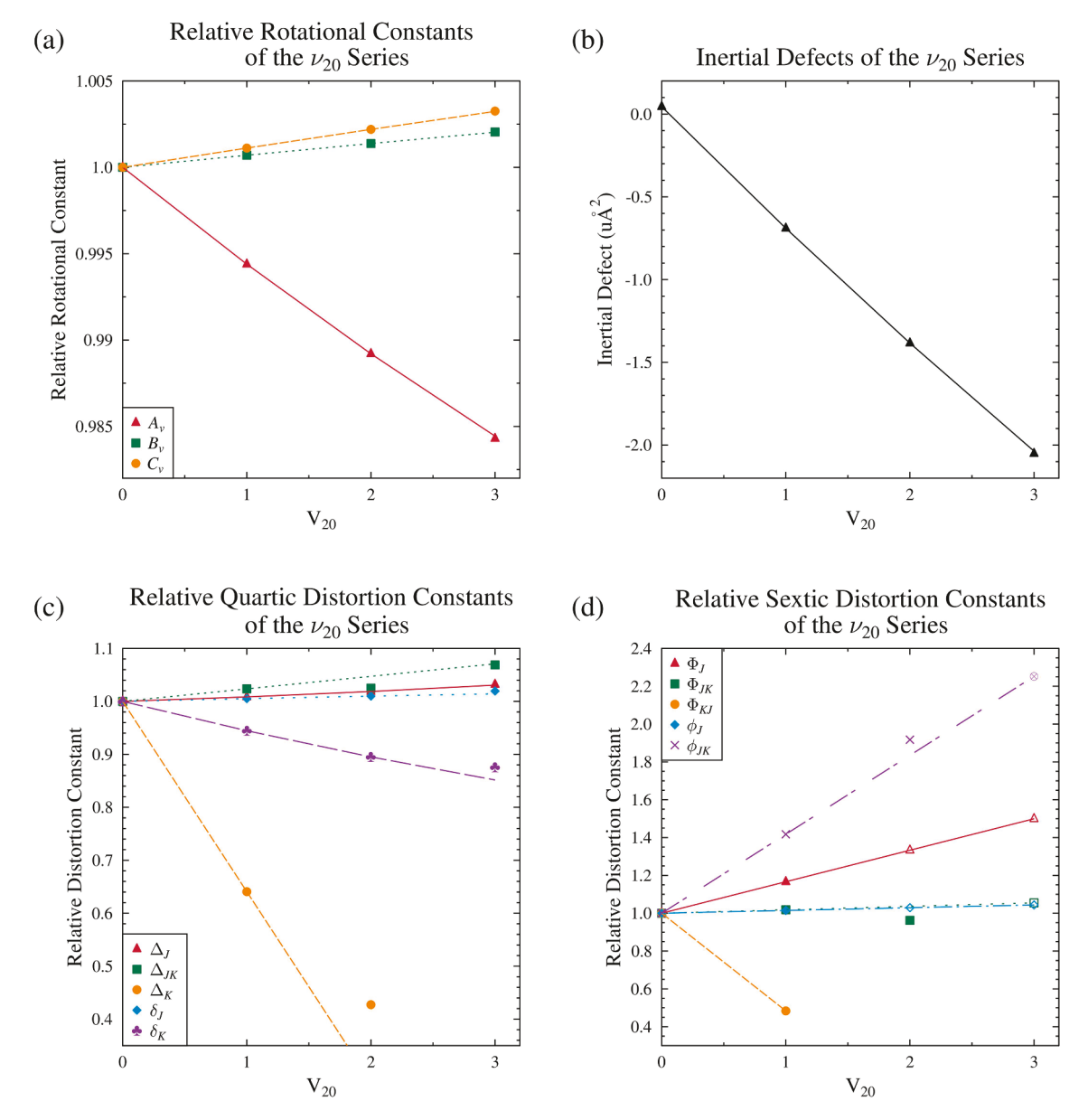


Fig. 6. (a) Relative rotational constants, (b) inertial defect, (c) relative quartic centrifugal distortion constants, and (d) relative sextic centrifugal distortion constants for the ν_{20} vibrational series of [35 Cl]-chlorobenzene as a function of vibrational excitation (v = 0, 1, 2, 3). Open symbols represent points held constant at their extrapolated values in their least-squares fits.

extrapolation of the parameters of the $v\nu_{30}$ series. The $2\nu_{30}$ overtone resides among five other vibrational states in the 586–616 cm⁻¹ range, and its $K_a = 0$ transitions appear to be strongly affected by Coriolis coupling at high J. At the point where increasing K_0 series begin to lose their K_c degeneracy (the transition from prolate- to oblate-top behavior), perturbation becomes more intense and fewer series can be included in the fit. The Δ_K parameter and all the sextic distortion terms needed to be held constant at the corresponding extrapolated values. Fig. 7 presents the trend in the spectroscopic constants for the v_{30} vibrational series (v = 0, 1, 2) and demonstrates linear changes in the relative rotational constants and inertial defects as a function of vibrational excitation. The trends for all of the quartic distortion terms are non-linear with increasing vibrational quanta. Holding one of the quartic centrifugal distortion constants at its extrapolated value did not result in the other quartic terms falling closer to linearity. Additionally, holding any of these terms constant at their extrapolated values required the exclusion of additional properly assigned rotational transitions. The deviation of the distortion constants from near-linearity indicates that the constants are absorbing the effects of unaddressed Coriolis-coupling in the single-state Hamiltonian, making the physical meaningfulness of these values dubious.

3.4. [35 Cl]-Chlorobenzene, ν_{11} and ν_{14}

The third excited fundamental of chlorobenzene, v_{11} (A_1 , $403 \, \mathrm{cm}^{-1}$), is a ring distortion with asymmetric C–C bond bending. Transitions in v_{11} were successfully identified using the experimental ground-state constants modified by the B3LYP/6–311+G(2d,p) vibration–rotation interaction constants. Although this state is at $403 \, \mathrm{cm}^{-1}$, and transitions are predicted to have only 14% of the ground-state intensity, about 2700 total transitions could still be measured. The values of Φ_{KJ} and Φ_K were unable to be determined and were instead held constant at their respective ground-state values. The $C_0 - C_{11}$ constant is in excellent agreement with the experimental value, but the predicted $A_0 - A_{11}$ and $B_0 - B_{11}$ constants exhibit larger deviations from experiment ($A_0 - A_{11}$ obs. - calc. = 2.23 MHz, 96.0%; $B_0 - B_{11}$ obs. - calc. = 0.25 MHz, 31.2%).

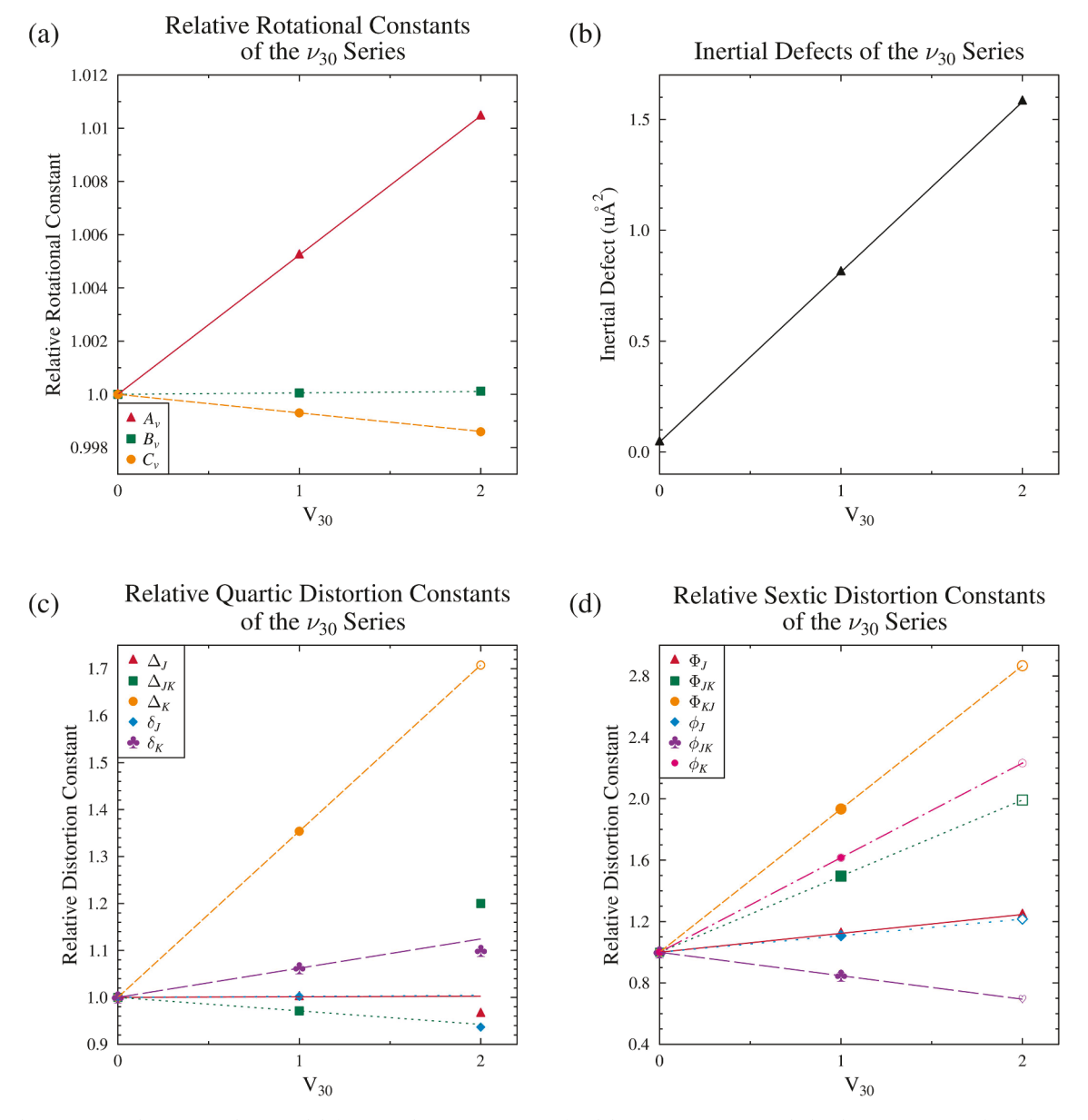


Fig. 7. (a) Relative rotational constants, (b) inertial defect, (c) relative quartic centrifugal distortion constants, and (d) relative sextic centrifugal distortion constants for the ν_{30} vibrational series of [35 Cl]-chlorobenzene as a function of vibrational excitation (v = 0, 1, 2). Open symbols represent points held constant at their extrapolated values in their least-squares fits.

The ν_{11} fundamental is 3 cm⁻¹ away from $2\nu_{20}$ and 13 cm⁻¹ away from ν_{14} . The predicted Coriolis-coupling constant between ν_{11} and ν_{14} ($|G_a|$ = 24.6 MHz), however, is small in magnitude relative to the size of the A rotational constant. The magnitudes of the coupling constants between $2\nu_{20}$ and these two fundamental vibrational states are expected to be small due to the large changes in vibrational quantum numbers, but, as mentioned above, the impact is noticeable on centrifugal distortion constants of $2\nu_{20}$ (vide infra). Large discrepancies between the computed and experimental A_0 – A_ν values were also observed in ν_{18} of 2-chloropyridine [17] and v_{16} of chloropyrazine [16] – two analogous molecules and states to v_{11} in chlorobenzene that will be reviewed in detail in the Discussion section. The fourth fundamental state, ν_{14} (A₁, 416 cm⁻¹), involves a stretch of the σ_{C-Cl} bond and ring atom along the same axis, making its theoretical prediction highly sensitive to the Cl-atom location. A total of 2724 transitions were located up to a $K_a = 46$. The vibration-rotation interaction constants for v_{14} are predicted with excellent success by the B3LYP calculation. The largest-magnitude difference between observed and calculated values is in A_0 – A_{14} (obs. –

calc.=0.19 MHz, 3.7% error), although the largest percent difference is in B_0-B_{14} (obs.-calc.=0.02 MHz, 7.3% error). All quartic and sextic constants were determined except Φ_{KJ} and Φ_{K} , which were held constant at the respective ground-state values.

3.5. [35 Cl]-Chlorobenzene, ν_{19} and $\nu_{20} + \nu_{30}$

The fifth excited fundamental of chlorobenzene, ν_{19} (B₁, 467 cm⁻¹), is a ring deformation ("butterfly" mode) bending the C=C-Cl angle with little motion of the chlorine atom. The ν_{19} state is not particularly close in energy to nearby states ($\nu_{14}=416$ cm⁻¹, $\nu_{20}+\nu_{30}=493$ cm⁻¹), but it is the first state with obvious visual perturbation in its rotational spectrum. Near $K_a=7$, transitions in the middle of otherwise well-predicted K_a series begin to slowly deviate from a distorted-rotor prediction. In a Loomis-Wood plot, frequencies with increasing values of J begin to progressively deviate from the prediction until reaching a maximally perturbed frequency. As the value of J continues to increase, the frequencies eventually return to a distorted-rotor prediction. The first

stants for 20

30 (A₂, 493 cm ¹), also contains individual combination state, 20 frequencies and entire series that cannot be treated with a distortedrotor Hamiltonian, beginning as early as K_a 0. A multistate analysis of 19 and 20 30 was attempted, but between the degree of coupling, vibrational-state intensity, and frequency overlap with other states, we were not able to fit enough data to determine spectroscopic constants or perturbation terms using this method. Instead, effective distorted-rotor fits of the vibrational states excluding obviously perturbed frequencies were obtained. Both $_{19}$ and $_{20}$ $_{30}$ have about 600 transitions in their respective least-squares fits. As a consequence of coupling combined with diminishing transition intensity, there is a sudden, substantial decrease in the total number of transitions, relative to the fits of lowerenergy vibrational states (ca. 2000 transitions). It is worth noting that a similar drop in transition count was observed in the analogous states of chloropyrazine and 2-chloropyridine and may imply those states experience similar coupling and intensity issues in their rotational spectra [16,17]. For 19, the predicted vibration rotation interaction constants are in excellent agreement with the final experimental values, with the largest uncertainty occurring in A_0 A_{19} (obs. calc. 40.5%) a reasonable error compared to previously studied monochlorinated aromatics [16,17]. The value of $_{K}$ in $_{19}$ was held constant at its ground-state value in the least-squares fitting to prevent other spectroscopic constants from becoming the wrong sign and order of magnitude in the least-squares fitting output. Only the $_J$ and $_{JK}$ 19 sextic distortion constants were allowed to vary; the remaining sextic terms were held constant at their respective ground-state values. For 20 30 and all other combination states, the extrapolated estimates of the spectroscopic constants from the experimental fundamental values allow for the easy identification of combination states, as well as a lower fit uncertainty. All of the quartic and one of the sextic distortion con-

3.6. [³⁵Cl]-Chlorobenzene: 20 11, 29, and 20 14

constants were held fixed at the extrapolated values.

The second-lowest combination state in chlorobenzene is 20 (B₂, 603 cm⁻¹), which is followed in energy by the sixth excited fundamental state 29 (B2, 615 cm 1). The 29 mode is an in-plane ringdeformation mode that is closely followed by another combination state, $_{14}$ (B₁, 616 cm 1). The intensities of the $_{20}$ $_{11}$, $_{29}$, and $_{20}$ 14 modes are all about 5% that of the ground state, and there are about 400 500 transitions in each of their data sets. The predicted A_0 A_{29} constant differs from the experimental value by 1.08 MHz, although the largest percent error is in the small shift of B_0 B_{19} (obs. calc. MHz, 55.7%). With 2 30 and 3 20, these five vibrational states comprise a complicated polyad of relatively weak Coriolis-coupling interactions, likely causing the observed effects in their rotational spectra and the inconsistency between the B3LYP-predicted and experimental constants in 29. The agreement between the extrapolated and experimental spectroscopic constants for combination states will be discussed further in the Discussion section.

 $_{30}$ ($_{J}$) could be fit, while the remaining spectroscopic

The fourth combination state in chlorobenzene is $_{20}$ $_{19}$ (A₁, 667 cm 1), which is followed in order of ascending energy by $_{18}$ (B₁, 685.59 cm 1) and 2 $_{20}$ $_{30}$ (B₁, 693 cm 1). The $_{18}$ vibration the seventh and last fundamental observed for [35 Cl]-chlorobenzene in this work involves in-plane ring deformation, with substantial motions of the *ortho* and *meta* carbon atoms. For the states near 700 cm 1 , the spectrum approaches the limit of spectral confusion, resulting in a substantial drop in the number of assignable transitions (368 in $_{20}$ $_{19}$, 90 in $_{18}$, 76 in 2 $_{20}$ $_{30}$). Because many constants needed to be held at fixed values for states with few transitions, the predicted and experimental vibration rotation interaction constants for $_{18}$ display only moderate agreement.

3.8. [37Cl]-Chlorobenzene, vibrational ground state

The ground state of [37Cl]-chlorobenzene has over 4600 independent frequency measurements assigned in its rotational spectrum over the 2 360 GHz region. The intensities of the ground-state transitions were consistent with the isotopic ratio of 3:1 for [35Cl] to [37Cl]-chlorobenzene. Due to the weaker spectral intensity, the vibrational ground state of the [37Cl] isotopologue contains fewer rotational transitions in the least-squares data set, and the frequency assignments are more likely to be impacted by the accidental overlap with other, more intense, vibrational series of the [35Cl] isotopologue. The rotational and quartic distortion constants agree to several decimal places with the previously determined experimental values (Table 4), but the uncertainties in the reported values do decrease somewhat [1.4 7]. There is excellent agreement between the predicted and experimental constants; A_0 , B_0 , and C_0 are predicted within 0.005%, 1.3%, and 1.0% of their experimental values, respectively. The B3LYP-computed quartic distortion constants agree in sign and order-of-magnitude with the experimental values, and the largest error is in κ (3.2%). Sextic distortion constants of the [37 Cl]-isotopologue ground state, except $_{K}$, are determined experimentally for the first time and are well-predicted by the B3LYP calculation, with differences ranging from 6.2% (in $_{IK}$) to 40.3% (in $_{JK}$). The $_{aa}$, $_{bb}$, and $_{cc}$ terms are experimentally determined, along with the nuclear spin-rotation constant $(M_{bb} M_{cc})/2$, and all are in excellent agreement with the previously reported values [1,4 6] and the B3LYP prediction (Table 4). Like the ground state of the [35Cl]-isotopologue, the addition of many hyperfine-resolved microwave transitions and thousands of unresolved millimeter-wave transitions slightly increases the precision and reduces uncertainty in each of the quadrupole coupling constants, as well as the nuclear spin-rotation constant.

3.9. [³⁷Cl]-Chlorobenzene, ₂₀ (v 1, 2)

Near 3100 transitions were measured, assigned, and least-squares fit with low error ($_{total\ fit}$ 0.033 MHz) for the $_{20}$ vibrationally excited state of [37Cl]-chlorobenzene, which has a calculated intensity of 13% of the [35 Cl]-isotopologue ground-state intensity. The $_{KJ}$ and $_{K}$ terms could not be determined and were held fixed to the respective groundstate values. When comparing a B3LYP prediction of the vibration rotation interaction constants for the [37Cl]-isotopologue to the experimental values, the largest error for $_{20}$ is in A_0 A_{20} (obs. calc. 0.64 MHz (2.0%)) an error nearly identical to the analogous 20 state of the [35 Cl]-isotopologue. The overtone vibration, 2 $_{20}$, is calculated to only be 4.5% of the [35Cl]-isotopologue ground-state intensity, and it is predicted to be only 3 cm $^{-1}$ from its nearest vibrational neighbor, $_{11}$. Like the 2 $_{20}$ state of [35 Cl]-chlorobenzene, similar deviations from distorted-rotor frequencies are present. Nevertheless, 2026 transitions were measured and included in the least-squares fit. The values of KJ, K, and K were not determinable and were held fixed to extrapolated values. The value of J converged to a value well off of the extrapolation, so it was held constant at its extrapolated value as well. The relative rotational constants for the vibrational series of $\ _{20}$ are displayed in Fig. 8. Unlike the $_{20}$ series of [35 Cl]-chlorobenzene, only the b- and caxis moments of inertia and relative rotational constants for the [37Cl]isotopologue display nearly linear changes as a function of vibrational state. A substantial amount of the untreated coupling is being absorbed by the A_{ν} and centrifugal distortion constants for 2 $\,_{20}$. Improvements in the determination of A_{ν} were not achieved by further constraining the centrifugal distortion constants to their extrapolated values. The resulting spectroscopic constants of 2 20 are somewhat effective and their physical meaning is questionable. In contrast, the spectroscopic constants of 20 are much more reliable and likely to be physically meaningful.

Table 4Spectroscopic constants for [³⁷Cl]-chlorobenzene in its ground and its vibrationally excited states (A-reduced Hamiltonian, I^r representation).

	B3LYP ^a	[³⁷ Cl] G.S. [1]	[³⁷ Cl] G.S. ^b	20	30
				B ₁ , 200 cm ^{1 c}	B ₂ , 293 cm ^{1 c}
$A_{\nu}^{(A)}$ (MHz)	5672	5672.2784 (52)	5672.27476 (82)	5640.2143 (15)	5702.2063 (20)
$B_{\nu}^{(A)}$ (MHz)	1513	1532.788668 (66)	1532.788685 (34)	1533.877446 (57)	1532.868572 (73)
$C_{\nu}^{(A)}$ (MHz)	1194	1206.574963 (63)	1206.574989 (33)	1207.923332 (51)	1205.734146 (60)
C _γ (WITE)	1174	1200.374703 (03)	1200.374707 (33)	1207.723332 (31)	1203.734140 (00)
_J (kHz)	0.057	0.0576980 (57)	0.0577449 (23)	0.0582469 (35)	0.0578186 (45)
_{JK} (kHz)	0.278	0.273615 (92)	0.273699 (19)	0.280233 (31)	0.265678 (60)
_K (kHz)	0.849	0.8785 (87)	0.8818 (17)	0.5553 (18)	1.2027 (26)
_J (kHz)	0.0133	0.0135679 (25)	0.0135867 (15)	0.0136625 (21)	0.0136182 (26)
_K (kHz)	0.296	0.29788 (22)	0.29899 (10)	0.28233 (14)	0.31819 (18)
$_{J}$ (mHz)	0.00164		0.002121 (99)	0.00313 (14)	0.00260 (18)
$_{JK}$ (mHz)	0.106		0.0962 (69)	0.1366 (40)	0.1534 (99)
_{KJ} (mHz)	0.529		0.491 (24)	[0.491] ^e	0.877 (48)
_K (mHz)	0.969		$[0.969]^{d}$	[0.969] ^e	[0.969] ^e
$_{J}$ (mHz)	0.00105		0.001164 (55)	0.001483 (73)	0.001368 (93)
$_{JK}$ (mHz)	0.0590		0.0536 (45)	0.1027 (54)	0.0544 (72)
$_{K}$ (mHz)	1.53		1.40 (13)	2.022 (82)	2.59 (18)
			= (4 1= 0 (O4))		
_{aa} (MHz)	53.8	56.1445 (16)	56.1452 (21)		
_{bb} (MHz)	29.6	30.1200 (27)	30.1198 (23)		
cc (MHz)	24.2	26.0244 (27)	26.0254 (45)		
g ,	0.1006	0.072948 (69)	0.072925 (90)		
M_{aa} (kHz) h	0.402				
$(M_{bb} M_{cc})/2 \text{ (kHz)}^{h}$	0.428	0.468 (89)	0.527 (100)		
$N_{ m lines}$ i		279	4673	3106	2455
		2/9	0.032	0.033	0.038
total fit (MHz)		0.760			
w.fit ^j _i (uÅ ²) ^k		0.763 0.045792 (86)	0.635 0.045729 (19)	0.667 0.694231 (32)	0.752 0.822686 (41)
[(m1)		2 20	010 107 25 (15)	0103 (201 (02)	
			1		11 A 400 1 c
· (A)		A ₁ , 400 c			A ₁ , 403 cm ^{1 c}
$A_{\nu}^{(A)}$ (MHz) $B_{\nu}^{(A)}$ (MHz)		5610.946 1534.918			5669.610 (71) 1531.9999 (56)
$C_{\nu}^{(A)}$ (MHz)		1209.213			1206.18115 (11)
C _γ (WIT IZ)		1205.213	52// (09)		1200.16113 (11)
_J (kHz)		0.058	38862 (17)		0.057568 (95)
_{JK} (kHz)			3642 (64)		[0.273699] e
K (kHz)			66 (20)		[0.8818] ^e
_J (kHz)			37449 (26)		0.013487 (47)
K (kHz)			787 (14)		0.2912 (17)
$_{J}$ (mHz)		[0.004			[0.002121] e
_{JK} (mHz)			50 (34)		[0.0962] ^e
$_{KJ}$ (mHz)		[0.491	-		[0.491] ^e
_K (mHz)		[0.969			[0.969] ^e
$_{J}$ (mHz)			2220 (78)		[0.001164] ^e
$_{JK}$ (mHz)			52 (46)		[0.0536] ^e
$_{K}$ (mHz)		[2.64]	j		[1.40] ^e
$N_{ m lines}$ i		2026			227
		0.041			0.045
total fit (MHz)		0.041			0.891
w.fit j		0.82/			0.091

1.384571 (44)

3.10. $[^{37}Cl]$ -Chlorobenzene: $_{30}$ and $_{11}$

 $_{i}$ (uÅ 2) k

The $_{30}$ and $_{11}$ fundamental states of [37 Cl]-chlorobenzene were located using the B3LYP-predicted vibration rotation interaction constants to modify the experimental [37 Cl]-chlorobenzene ground-state

spectroscopic terms. Over 2450 transitions were included for the final $_{30}$ fit, allowing for the determination of all but the $_K$ distortion constant. The predicted and experimental vibration rotation interaction terms are in excellent agreement for $_{30}$, with the largest error in A_0 A_{30} (obs. calc. 0.57 MHz, 1.9%). The $_{11}$ state, on the other hand,

0.0291 (16)

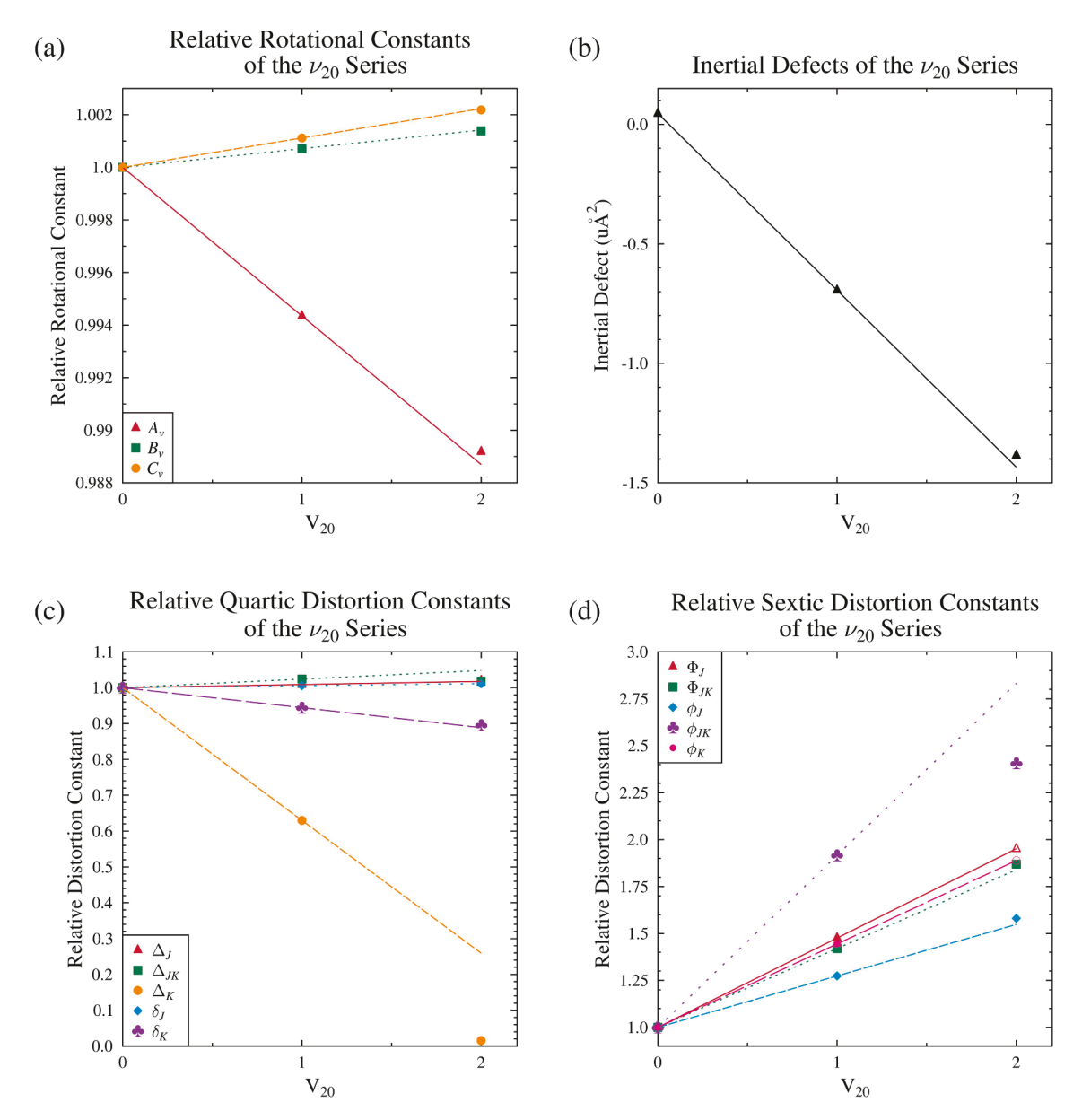


Fig. 8. (a) Relative rotational constants, (b) inertial defect, (c) relative quartic centrifugal distortion constants, and (d) relative sextic centrifugal distortion constants for the ν_{20} vibrational series of [37 Cl]-chlorobenzene as a function of vibrational excitation (v = 0, 1, 2). Open symbols represent points fixed to their extrapolated values in their least-squares fits.

displays a large discrepancy between predicted and experimental values in both $A_0 - A_{11}$ (obs. – calc. = 2.54 MHz, 95.5%) and $B_0 - B_{11}$ (obs. – calc. = 0.24 MHz, 30.6%). The ν_{11} state of [35 Cl]-chlorobenzene, however, deviates from its predicted values by the same amount. Considering only 227 transitions could be included for v_{11} , it is unsurprising that only three distortion constants could be determined. The v_{11} state of [³⁷Cl]-chlorobenzene suffers from intense overlap with several different vibrational states and, unlike the [35 Cl]-chlorobenzene ν_{11} analog, has obvious perturbation in its spectrum observed as early as $K_a = 4$, resulting from interaction with ν_{14} . Although well predicted, a number of high-error transitions were removed from the least-squares fit in order to prevent multiple sextic distortion terms from having the wrong sign or order of magnitude. The transition counts of v_{11} and other similar states will be discussed in more detail in the following section. The [37Cl]chlorobenzene $2\nu_{20}$, ν_{11} , and ν_{14} transitions are estimated to be between 4.2 and 4.5% as intense as the [35 Cl]-isotopologue ground state. Despite the fact that these three states are predicted to have similar intensity, 2030 transitions were assigned for the $2\nu_{20}$ state, 227 transitions were

measured for v_{11} , but no transitions could be assigned for v_{14} .

4. Discussion

The current investigation involving millimeter-wave rotational spectroscopy of vibrationally excited states of chlorobenzene, when combined with data from the analogous studies of 2-chloropyridine [17] and chloropyrazine [16], affords the opportunity for detailed comparisons of spectroscopic constants among these structurally related compounds. Comparing spectroscopic constants across a homologous series of molecules, in their ground vibrational states, is, of course, a routine matter. And structure–property relationships have long been probed by vibrational spectroscopy. Comparing spectroscopic constants for vibrationally excited states of structurally related compounds, however, is quite rare. In fact, we are not aware of previous comparisons of such extensive data sets.

The differences in rotational and quartic distortion constants between the ground state and vibrationally excited states of many

Journal of Molecular Spectroscopy 394 (2023) 111//c

Table 5Change in spectroscopic constants upon analogous vibrational excitation of the ³⁵Cl isotopologues of chlorobenzene, 2-chloropyridine, and chloropyrazine (A-reduction, I^r representation).

	chlorobenzene	2-chloropyridine	chloropyrazine	chlorobenzene	2-chloropyridine	chloropyrazine
	₂₀ , 200 cm ¹	₂₇ , 187 cm ¹	₂₄ , 188 cm ¹	30, 293 cm ¹	₁₉ , 312 cm ¹	₁₇ , 309 cm ¹
A_{ν} (MHz)	31.8067 (10)	28.46757 (29)	28.6336 (22)	29.6862 (14)	25.41823 (34)	25.1066 (21)
$B_0 = B_v \text{ (MHz)}$	1.106602 (48)	1.160625 (32)	1.117171 (83)	0.085313 (54)	0.002367 (45)	0.11538 (50)
$C_0 = C_v \text{ (MHz)}$	1.378610 (46)	1.524539 (33)	1.5830008 (77)	0.859662 (49)	1.016241 (40)	0.95435 (40)
$_{J})_{0}$ ($_{J})_{\nu}$ (Hz)	0.5098 (32)	0.5880 (15)	0.6105 (16)	0.0731 (38)	0.1261 (20)	0.1668 (16)
JK) ₀ (JK) _{V} (Hz)	6.661 (21)	3.929 (23)	3.189 (27)	8.094 (27)	4.603 (46)	5.415 (50)
	313.0 (14)	191.07 (34)	193.8 (31)	308.2 (21)	199.86 (29)	216.3 (34)
$(K)_0 (K)_V (Hz)$		0.0778 (18)			' '	
$(J)_0$ $(J)_v$ (Hz)	0.0749 (20)	7 7	0.077 (23)	0.0314 (22)	0.0292 (22)	0.0469 (95)
$_{K})_{0}$ ($_{K})_{\nu}$ (Hz)	17.04 (14)	12.271 (54)	12.94 (15)	19.13 (16)	15.254 (91)	16.60 (16)
	2 ₂₀ , 400 cm ¹	2 ₂₇ , 374 cm ¹	2 ₂₄ , 376 cm ¹	11, 403 cm ¹	₁₈ , 407 cm ¹	₁₆ , 435 cm ¹
$A_0 = A_{\nu} \text{ (MHz)}$	61.2286 (14)	55.96024 (38)	56.5228 (19)	2.3254 (17)	0.6355 (19)	0.3721 (23)
B_{ν} (MHz)	2.176340 (54)	2.312298 (42)	2.233578 (70)	0.792995 (69)	1.351208 (89)	1.530827 (74
$C_0 = C_v \text{ (MHz)}$	2.710776 (49)	3.038999 (39)	3.161557 (61)	0.417354 (61)	0.702229 (69)	0.842222 (66
$_{J})_{0}$ ($_{J})_{\nu}$ (Hz)	1.1246 (38)	1.1964 (20)	1.2365 (16)	0.2263 (49)	0.5320 (65)	0.5584 (19)
$_{JK})_0$ ($_{JK})_v$ (Hz)	7.003 (27)	6.377 (40)	5.737 (41)	3.651 (49)	2.517 (87)	1.344 (34)
$(K)_0 (K)_{\nu} (Hz)$	496.1 (21)	355.28 (30)	368.2 (26)	141.0 (24)	5. (43)	27.4 (31)
$_{J})_{0}$ ($_{J})_{\nu}$ (Hz)	0.1545 (22)	0.1541 (21)	0.1538 (20)	0.0836 (28)	0.1525 (39)	0.1660 (21)
$_{K})_{0}$ ($_{K})_{\nu}$ (Hz)	32.39 (16)	24.087 (82)	25.18 (11)	2.39 (20)	2.198 (92)	0.78 (12)
	₁₄ , 416 cm ¹	₂₆ , 407 cm ¹	₂₃ , 413 cm ¹	₁₉ , 467 cm ¹	₂₅ , 481 cm ¹	₂₂ , 477 cm ¹
$A_0 = A_{\nu} \text{ (MHz)}$	5.1580 (17)	5.24054 (45)	4.5727 (21)	1.141 (23)	0.995 (23)	1.505 (55)
B_{ν} (MHz)	0.252459 (75)	0.261308 (63)	0.161208 (75)	0.1825 (23)	0.1915 (22)	0.0043 (46)
	0.705149 (62)	0.763409 (49)	0.740198 (64)	0.584035 (95)	0.53013 (11)	0.682660 (84
$_{J})_{0}$ ($_{J})_{\nu}$ (Hz)	0.1435 (48)	0.2028 (32)	0.1783 (19)	0.08 (16)	0.984 (58)	1.75 (25)
$_{JK})_0$ ($_{JK})_v$ (Hz)	0.077 (42)	0.01 (10)	0.283 (65)	11.1 (65)		77. (11)
$_{K})_{0}$ ($_{K})_{\nu}$ (Hz)	10.8 (22)	0.64 (34)	3.7 (28)	0.006 (00)	0.000 (40)	0.00 (10)
$_{J})_{0}$ ($_{J})_{v}$ (Hz) $_{K})_{0}$ ($_{K})_{v}$ (Hz)	0.0174 (30) 0.48 (19)	0.0389 (30) 1.87 (11)	0.0290 (21) 0.98 (11)	0.006 (83) 3.6 (13)	0.338 (40) 23.6 (13)	0.98 (12) 9.6 (22)
	₂₀ ₃₀ , 493 cm ¹	₂₇ ₁₉ , 499 cm ¹	₂₄ ₁₇ , 497 cm ¹	3 ₂₀ , 600 cm ¹	3 ₂₇ , 561 cm ¹	3 ₂₄ , 564 cm ¹
$A_0 = A_{\nu} \text{ (MHz)}$	2.4932 (30)	1.85 (39)	3.232 (58)	89.064 (14)	82.608 (22)	83.6742 (94)
B_{ν} (MHz)	1.17637 (23)	0.894 (32)	1.0573 (48)	3.2301 (13)	3.4595 (22)	3.34519 (91)
C_{ν} (MHz)	0.531186 (82)	0.53960 (12)	0.636966 (83)	4.017543 (79)	4.545263 (67)	4.735640 (68)
$_{J})_{0}$ ($_{J})_{\nu}$ (Hz)	0.684 (24)	0.40 (12)	1.45 (37)	1.944 (54)	1.731 (34)	1.618 (45)
$_{JK})_0$ ($_{JK})_{\nu}$ (Hz)	4.9 (22)	0.10 (12)	27. (15)	18.5 (23)	11, 61 (61)	14.7 (19)
$(K)_0 (K)_v (Hz)$	158. (29)		27. (10)	10.5 (25)		11.7 (15)
$J_0 = \begin{pmatrix} \chi \rangle_V \text{ (Hz)} \\ J_0 = \begin{pmatrix} \chi \rangle_V \text{ (Hz)} \end{pmatrix}$	0.180 (12)	0.014 (59)	0.50 (18)	0.313 (28)	0.183 (17)	0.100 (22)
$(K)_0$ $(K)_v$ (Hz)	0.8 (12)	6.3 (26)	4.7 (28)	38.76 (54)	37.46 (57)	36.89 (45)
K)0 (K)ν (HZ)	0.8 (12)	0.3 (20)	4.7 (28)	38.70 (34)	37.40 (37)	30.69 (43)
	20 11, 603 cm ¹	₂₇ ₂₆ , 594 cm ¹	24 23, 601 cm ¹	₂₉ , 615 cm ¹	₁₇ , 618 cm ¹	₁₅ , 618 cm ¹
A_{ν} (MHz)	37.727 (13)	33.278 (86)	35.42 (58)	7.003 (10)	1.71 (18)	0.65 (23)
B_{ν} (MHz)	0.3643 (12)	1.4310 (75)	2.452 (46)	0.0644 (10)	0.076 (15)	0.343 (19)
$C_0 = C_v \text{ (MHz)}$	1.03818 (10)	2.265840 (93)	2.21827 (11)	0.857398 (90)	0.914027 (82)	0.82723 (12)
$_{J})_{0}$ ($_{J})_{\nu}$ (Hz)	0.173 (21)	0.831 (59)	1.09 (61)	3.162 (86)	1.125 (72)	1.04 (10)
JK) ₀ (JK) _{ν} (Hz)	• •		17. (18)	120.5 (36)	• /	,
$(K)_0$ $(K)_v$ (Hz)						
$_{J})_{0}$ ($_{J})_{\nu}$ (Hz)	0.028 (10)	0.117 (29)	0.09 (30)	1.495 (44)	0.167 (61)	0.527 (50)
$(K)_0 (K)_V (Hz)$	35.08 (39)	12.7 (10)	0.07 (00)	24.88 (78)	36.629 (18)	18.3 (20)
KJU (KJy (112)	33.00 (33)	12.7 (10)		24.00 (70)	30.027 (10)	
						(continued on next page

	2 30, 586 cm ¹	2 ₁₉ , 624 cm ¹	2 ₁₇ , 618 cm ¹	20 14, 616 cm 1	27 18, 594 cm ¹	24 16, 623 cm ¹
$A_0 A_{\nu} (MHz)$	59.207 (34)		50.15 (18)	36.061 (52)	30.94 (41)	31.07 (13)
$B_0 = B_V \text{ (MHz)}$	0.1990 (31)	0.0137 (13)	0.233 (14)	1.3283 (47)	0.168 (33)	0.345 (11)
$C_0 - C_V \text{ (MHz)}$	1.733765 (84)	2.00144 (10)	1.931570 (85)	2.06058 (10)	0.84335 (11)	0.75331 (14)
$(J_0 (J_v(Hz))$	1.35 (26)	0.41 (12)	0.75 (24)	0.05 (47)	0.61 (30)	0.98 (42)
$(\ _{\mathcal{R}})_0 \ (\ _{\mathcal{R}})_v (\mathrm{Hz})$ $(\ _{\mathcal{R}})_0 \ (\ _{\mathcal{R}})_v (\mathrm{Hz})$	26. (11)		18.9 (74)	50. (19)		70. (13)
(j_0)	0.56 (13)	0.058 (61)	0.32 (12)	0.39 (24)	0.02 (14)	0.84 (20)
$(\kappa)_0 (\kappa)_\nu$ (Hz)	29.5 (23)	4.1 (18)		6.5 (35)	22.6 (50)	
	20 19, 667 cm ¹	27 25, 668 cm ¹	24 22, 665 cm ¹	2 20 30, 693 cm ¹	2 ₂₇ ₁₉ , 686 cm ¹	2 24 17, 685 cm ¹
$A_0 A_\nu \text{ (MHz)}$	33.0057 (91)	30.41 (16)	30.34 (40)	31.2 (11)		32.2940 (29)
$B_0 - B_{\nu} \text{ (MHz)}$	0.9361 (10)	1.179 (13)	1.131 (32)	2.155 (88)	1.9649 (18)	1.25308 (10)
C ₀ C _v (MHz)	1.944375 (80)	2.01945 (12)	2.26176 (12)	1.87280 (42)	2.08303 (12)	2.270068 (78)
$(J_0 (J_v(Hz))$	1.02 (12)	1.11 (17)	2.52 (49)	2.11 (73)	0.50 (14)	0.8768 (59)
$(J_{R})_{0}$ $(J_{R})_{\nu}$ (Hz)	4.8 (48)		126. (15)			0.797 (95)
$(\kappa)_0 (\kappa)_\nu$ (Hz)						116.2 (69)
$(J)_0 (J)_\nu (Hz)$	0.298 (59)	0.281 (86)	1.61 (24)	0.81 (36)	0.188 (74)	0.0800 (36)
$(\kappa)_0 (\kappa)_\nu$ (Hz)	15.0 (11)	0.9 (31)		6. (13)	28.2 (22)	11.38 (18)

analogous modes of the [35Cl]-isotopologues of chlorobenzene, 2-chloropyridine [17] and chloropyrazine [16] are provided in Table 5. The consistency of the experimental differences across the three molecules is not unexpected due to the similar molecular structures and vibrational motions of the atoms. The spectroscopic constants of the first set of vibrationally excited states in chlorobenzene (20), 2-chloropyridine (27), and chloropyrazine (24) all exhibit differences from their respective ground states that are equal in sign and order-of-magnitude. In these first excited states, the experimental and B3LYP-predicted vibration rotation interaction constants for each molecule display good agreement. The second set of vibrationally excited states in chlorobenzene ($_{30}$), 2-chloropyridine ($_{19}$), and chloropyrazine ($_{17}$) exhibit differences from their respective ground states that are the same orderof-magnitude, and, with one exception, equal in sign. The exception, the values of B_0 B_{v} , are among the smallest values in the table and all have magnitudes 120 kHz. Similarly, there are no major deviations between experimental and B3LYP-computed vibration rotation interaction terms (Table 3, [16,17]).

Depending on the chloroarene, the energy ordering of the next two fundamental vibrational modes may be exchanged due to their small energy differences, but, in each case, they involve the $_{\rm C}$ Cl bond stretching mode and the ring distortion mode with asymmetric C C bond bending. In the three analogous vibrational modes involving out-of-plane ring deformations ($_{11}$, $_{18}$, and $_{16}$ for chlorobenzene, 2-chloropyridine, and chloropyrazine, respectively), the A_0 A_V constants deviate from each other by as much as 2 MHz. The B3LYP-computed A_0

 A_{ν} constants were sufficiently different from the final experimental values that the assignment of these vibrationally excited states was challenging and relied on a combination of spectral intensities and their rotational constants. Complicating the interpretation of these discrepancies, the B3LYP-computed A_0 A_{ν} constants for the analogous vibrational states of all three cyanoarenes are predicted to be fairly small in magnitude, with the largest having an absolute value of 0.44 MHz. Additionally, there are substantial differences in the centrifugal distortion constants for these three vibrationally excited states, particularly for $(K)_0$ $(K)_v$, for which the values differ by two orders of magnitude. In contrast, the shifts in the rotational constants for the C Cl bondstretching and in-plane ring deformation modes ($_{14}$, $_{26}$, and $_{23}$ for chlorobenzene, 2-chloropyridine, and chloropyrazine, respectively) are nearly equal. In that set of vibrationally excited states, the predicted and experimental vibration rotation interaction terms are also in excellent agreement. The changes in the K-dependent quartic distortion constants for this set of vibrationally excited states, $(K)_0$ $(K)_v$, and $(K)_0$ $(K)_v$, show more variation in sign and magnitude than the other *J*-dependent centrifugal distortion constants. The molecular symmetry of each chloroarene allows for a-type Coriolis coupling to occur between vibrational states, which may be responsible for the deviations observed in the A_0 A_{ν} values. Treatment of the a-axis Coriolis coupling was attempted via a two-state Hamiltonian with their near-energy vibrational states (14, 26, and 23 for chlorobenzene, 2-chloropyridine, and chloropyrazine, respectively). The predicted Coriolis-coupling constants, however, are fairly small in magnitude (chlorobenzene $|G_a^{11}|^{14}$

24 6 ; 2-chloropyridine $\left|G_a^{18\,26}\right|$ 351 9 , $\left|G_b^{18\,26}\right|$ 21 7 ; chloropyrazine $\left|G_a^{16\,23}\right|$ 143 , $\left|G_b^{16\,23}\right|$ 91 8). Commonly, the A_0 A_ν values have large, oppositely signed values when the Coriolis coupling between two states has not been adequately treated. This characteristic was not observed for the untreated dyad of $_{11}$ and $_{14}$ in chlorobenzene, nor was it observed in the analogous vibrational states of chloropyrazine or 2-chloropyridine. Even in 2-chloropyridine [17], which has both the largest predicted Coriolis-coupling constants and vibrational states with nearly degenerate vibrational energies ($_{18}$, A, 407 cm 1 and $_{26}$, A, 407 cm 1), the Coriolis interaction was insufficient to generate large perturbations. An attempt to fit the transitions of

these vibrational states as a coupled dyad, however, resulted in only

small values of the coupling terms, with uncertainties larger than the values of the terms, themselves. All three of these dyads are similarly close in energy to the first overtones (2 $_{20}$, 2 $_{27}$, and 2 $_{24}$ for chlorobenzene, 2-chloropyridine, and chloropyrazine, respectively). A triad treatment involving Coriolis and Fermi couplings has not been attempted for any of these systems, as no largely perturbed or resonant transitions have been observed. These observations support the inference that some untreated coupling is being absorbed by the A_{v} -rotational constant and centrifugal distortion constants of all of these vibrationally excited states. As the changes with respect to the ground state for all constants are reasonable for a well-treated vibrationally excited state, it is only by comparison between analogous states for the chloroarenes and by the somewhat irregular behavior of the $_{20}$, $_{27}$, and $_{24}$ series for chlorobenzene, 2-chloropyridine, and chloropyrazine, respectively, that the likely presence of untreated coupling is revealed.

The fifth set of analogous fundamental vibrational states (19, 25, and 22 for chlorobenzene, 2-chloropyridine, and chloropyrazine, respectively) are out-of-plane, ring-deformation modes; the differences in spectroscopic constants do not substantially deviate from one another and there is minimal disagreement between the B3LYP-computed and experimental values. This behavior is consistent with these states being well isolated in energy from the other fundamentals in each chloroarene and having minimal coupling interactions with the nearby overtone and combination states. The sixth set of fundamental states compared in this work (29, 17, and 15 for chlorobenzene, 2-chloropyridine, and chloropyrazine, respectively) displays poor agreement between experimental spectroscopic constant changes relative to their respective ground states. Only the C_0 C_v constants maintain the same sign and have relatively small changes in the magnitude across all three chloroarenes. The agreement between the computed values and the experimental values for the vibration rotation interaction constants is good for 17 of 2-chloropyridine [17] and poor for $_{29}$ of chlorobenzene and $_{15}$ of chloropyrazine [16]. This can be attributed, in part, to the vibrational energies of these modes and other vibrationally excited states. There are no vibrationally excited states predicted within 10 cm ¹ of ₁₇ for 2-chloropyridine, but 29 of chlorobenzene and 15 of chloropyrazine each has a combination state ($_{20}$ $_{14}$ of chlorobenzene) or an overtone (2 $_{17}$ of chloropyrazine) that is nearly degenerate with it. The unaddressed coupling, allowed by the very close energy of these states, makes their experimental spectroscopic constants much less reliable. With the limited number of transitions available for the states above 600 cm $^{-1}$ in all of these works, a more insightful analysis is not feasible, nor is it likely that the interactions between vibrational states could be treated in the least-squares fit. It appears, however, given the good agreement between computed and experimental spectroscopic constants for 2-chloropyridine, that the poor agreement of the computed constants for the other two chloroarenes is due to questionably meaningful experimental values and not poorly modeled theoretical values. Though not presented in Table 5, a similar level of agreement between spectroscopic constants has been observed for the [37 Cl]-chloroarenes of the analogous vibrational modes. This analysis is available in the Supplementary Material.

The measurement, assignment, and least-squares fitting of five combination states of [35Cl]-chlorobenzene described above allows for an analysis of the changes in spectroscopic constants from two different vibrational modes. Such an analysis provides an additional validation of the physical meaningfulness of the spectroscopic constants, as the changes relative to the ground state should be approximately equal to the linear combination of the changes for each of the vibrational fundamentals. The spectroscopic constants of all observed combination states were extrapolated in this manner from the ground-state and corresponding vibrationally excited-state constants, as described previously for chloropyrazine [16] and 2-chloropyridine [17]. These extrapolations were useful in the initial assignment and least-squares fitting of the combination states. Where possible, these extrapolated values were allowed to vary as the data set increased in size. In each case, the values of some spectroscopic parameters could not be determined via leastsquares fitting and remained held at their extrapolated values. All the combination state obs. extr. values are reasonably small, and all the extrapolated rotational constants are within 0.06% of the experimentally determined value. Like the fundamental states, the largest overall obs. extr. values are typically in the A_{ν} and K-dependent distortion terms, and the differences are typically worse for vibrations mixing with energetically neighboring states. For the quartic distortion constants,

Table 6Experimentally determined spectroscopic constants and differences from linearly extrapolated predictions for combination states of [35Cl]-chlorobenzene (A-reduced Hamiltonian, I^r representation).^a

	[³⁵ Cl] ₂₀ ₃₀		[³⁵ Cl] ₂₀ ₁₁		[³⁵ Cl] ₂₀ ₁₄	
	A ₂ , 493 cm ^{1 b}	obs. extr.	B ₁ , 603 cm ^{1 b}	obs. extr.	A ₂ , 616 cm ^{1 b}	obs. extr.
$A_{\nu}^{(A)}$ (MHz)	5669.7845 (30)	0.37	5634.550 (13)	3.59	5636.216 (52)	0.90
$B_{\nu}^{(A)}$ (MHz)	1577.96305 (23)	0.016	1577.1510 (12)	0.051	1578.1150 (47)	0.031
$C_{\nu}^{(A)}$ (MHz)	1234.206200 (80)	0.012	1234.713201 (97)	0.077	1235.735599 (99)	0.023
$_{J}$ (kHz)	0.061013 (24)	0.00010	0.060503 (21)	0.00056	0.06038 (47)	0.00060
_{JK} (kHz)	0.2768 (22)	0.0034	[0.2910] ^c		0.332 (19)	0.044
K (kHz)	0.716 (29)	0.15	[0.4171] ^c		[0.5689] ^c	
$_{J}$ (kHz)	0.014666 (12)	0.000074	0.014458 (10)	0.00019	0.01410 (24)	0.00048
$_{K}$ (kHz)	0.3084 (12)	0.0013	0.27244 (38)	0.016	0.3140 (35)	0.023
	[³⁵ Cl] ₂₀ ₁₉		[³⁵ Cl] 2 ₂₀ ₃₀			
	A ₁ , 667 cm ^{1 b}	obs. extr.	B ₁ , 693 cm ^{1 b}	obs. extr.		
$A_{\nu}^{(A)}$ (MHz)	5639.2712 (91)	0.058	5641.1 (11)	2.75		
$B_{\nu}^{(A)}$ (MHz)	1577.72274 (96)	0.012	1578.942 (88)	0.14		
$C_{\nu}^{(A)}$ (MHz)	1235.619398 (78)	0.018	1235.54782 (42)	0.025		
$_{J}$ (kHz)	0.06135 (12)	0.00043	0.06244 (73)	0.0010		
_{JK} (kHz)	0.2865 (48)	0.013	[0.2869] ^c			
_K (kHz)	[0.5581] ^c		[0.5534] ^c			
$_{J}$ (kHz)	0.014784 (59)	0.00023	0.01530 (36)	0.00063		
$_{K}$ (kHz)	0.2925 (11)	0.0016	0.314 (13)	0.021		

^a Values for linearly extrapolated predictions provided in supplementary material. ^b Vibrational frequencies drawn from those measured in [25 28]. ^c Value held constant at the value extrapolated from ground and corresponding vibrational states.

the extrapolated values deviating the most are still within 22% of those determined experimentally (20 $_{30}$, $_{K}$), but many values are 1%. The extrapolated and experimental sextic distortion constants are within 30, J), although only a total three of these constants were determined for the combination states. Table 6 reproduces the spectroscopic constants alongside the differences between the observed and extrapolated values (obs. extr.). Given the precise and accurate spectroscopic constants determined for the ground state, 20, and 30, the 30 are expected to be quite good. The extrapolated constants for 20 spectroscopic constants of 20 30 and 20 19 are in much closer agreement with the extrapolated values than the other combination states. Inspection of the separation in vibrational energy of these vibrational states and their near-energy neighbors (Fig. 2.) shows that these states have greater energy separation to nearby vibrational states than the other combination states. For instance, the closest neighbor of 30 is 19, which has very well-behaved experimental spectroscopic constants, as discussed above. All of the other combination states have much smaller energy separations to other vibrationally excited states and have poorer agreement between the extrapolated and experimental spectroscopic constants. It is likely that the experimental constants for these states are being perturbed by unaddressed coupling, particularly 30. The experimental spectroscopic constants 11 and 2 20 presented for these states should be considered to be useful, but not completely accurate.

5. Conclusion

Transitions for a large number of vibrational states of chlorobenzene were assigned, measured, and least-squares fit in very dense spectra in this study and in similar studies of related chloroarenes [16,17]. The highest-energy vibrational state of [35Cl]-chlorobenzene included in this $_{30}$, has an easily identifiable K_a 0 series indicating that the detection limit for vibrationally excited states has not been reached. There is no inherent experimental reason why 18 and 30 states slightly higher in energy could not be assigned. It is possible that they will be identified in future work. This situation is consistent with similar studies of chloroarenes, where the limit to finding high-energy fundamentals is the ability to predict accurate vibration rotation interaction constants. In each of these works, extrapolation from experimental constants more accurately predicted the K_a 0 series at the high-energy limit of the states observed, allowing for their assignment. Their measurement and assignment of other vibrationally excited states would be greatly assisted by improved computational predictions and by better treatment of the expected coupling interactions with other near-energy vibrational states.

This work, in combination with the related studies of 2-chloropyridine and chloropyrazine, provides precise and accurate spectroscopic constants for many vibrationally excited states for their respective [³⁵Cl]- and [³⁷Cl]-isotopologues. Meaningful comparisons of the experimental and theoretical ground-state spectroscopic constants are readily accessible via common computational software packages. Examples of computationally predicted spectroscopic constants for vibrationally excited states, however, remain rather limited [44 48]. With the impact of state-mixing on the spectroscopic constants, it can often be difficult to evaluate the physical meaning of the experimental values obtained by least-squares fitting. With spectroscopic constants available for many vibrationally excited states for three related species, comparisons between analogous vibrationally excited states have been made. Careful comparison has validated the physical meaningfulness of spectroscopic constants for vibrationally excited states of chlorobenzene, 2chloropyridine, and chloropyrazine. These comparisons reveal subtle effects of coupling between states that were not fully appreciated in the previous works, somewhat reducing the expected accuracy of those experimentally determined spectroscopic constants. An experimental analysis to determine which spectroscopic constants are most reliable is important to allow meaningful benchmarking of computational methods as prediction of excited-state spectroscopic constants becomes more commonplace. The ability to computationally predict the spectroscopic constants for vibrationally excited states is important. As described above, these predictions often assist in the assignment and least-squares fitting of the rotational spectra of higher-energy fundamental vibrational states with lower populations.

Declaration of Competing Interest

The authors declare that they have no known competing financial interests or personal relationships that could have appeared to influence the work reported in this paper.

Data availability

Data are provided in the article and in the Supplementary Material.

Acknowledgments

We gratefully acknowledge funding from the National Science Foundation for support of this project (CHE-1664912 and CHE-1954270). P.M.D thanks the Graduate School, University of Wisconsin-Madison, for support as an Advanced Opportunity Fellow. P. B.C. and M.C.M. acknowledge support from the National Science Foundation (AST-1908576). We thank Maria Zdanovskaia for assistance in collecting the experimental millimeter-wave spectra.

Appendix A. Supplementary Material

Supplementary data to this article can be found online at https://doi.org/10.1016/j.jms.2023.111776.

References

- [1] O. Dorosh, E. Bia kowska-Jaworska, Z. Kisiel, L. Pszczó kowski, New measurements and global analysis of rotational spectra of Cl-, Br-, and I-benzene: spectroscopic constants and electric dipole moments, J. Mol. Spectrosc. 246 (2007) 228 232.
- [2] Z. Kisiel, E. Bia kowska-Jaworska, L. Pszczó kowski, The millimeter-wave rotational spectrum of fluorobenzene, J. Mol. Spectrosc. 232 (2005) 47 54.
- [3] Z. Kisiel, E. Bia kowska-Jaworska, Sextic centrifugal distortion in fluorobenzene and phenylacetylene from cm-wave rotational spectroscopy, J. Mol. Spectrosc. 359 (2019) 16–21.
- [4] R.L. Poynter, Microwave spectrum, quadrupolar coupling constants, and dipole moment of chlorobenzene, J. Chem. Phys. 39 (1963) 1962–1966.
- [5] W. Caminati, A.M. Mirri, Quadrupole hyperfine structure in the rotational spectrum of bromo- and chlorobenzene, Chem. Phys. Lett. 12 (1971) 127–130.
- [6] Z. Kisiel, The millimeter-wave rotational spectrum of chlorobenzene: analysis of centrifugal distortion and of conditions for oblate-type bandhead formation, J. Mol. Spectrosc. 144 (1990) 381–388.
- [7] A. Uskola, F.J. Basterretxea, F. Castaño, Diode-laser spectroscopy of the 19a band of chlorobenzene in a supersonic jet, J. Mol. Spectrosc. 202 (2000) 262 271.
- [8] J.L. Neill, S.T. Shipman, L. Alvarez-Valtierra, A. Lesarri, Z. Kisiel, B.H. Pate, Rotational spectroscopy of iodobenzene and iodobenzene neon with a direct digital 2 8 GHz chirped-pulse Fourier transform microwave spectrometer, J. Mol. Spectrosc. 269 (2011) 21 29.
- [9] M. Onda, T. Odaka, H. Miyazaki, M. Mori, I. Yamaguchi, Y. Niide, Microwave spectrum, quadrupole coupling constant tensors, and dipole moments of 1-chloro-3-fluorobenzene, J. Mol. Spectrosc. 165 (1994) 426–432.
- [10] M. Onda, T. Odaka, H. Miyazaki, M. Mori, I. Yamaguchi, Y. Niide, Microwave spectrum, quadrupole coupling constants, and dipole moments of 1-chloro-2fluorobenzene, J. Mol. Spectrosc. 176 (1996) 17 22.
- [11] Z. Kisiel, E. Bia kowska-Jaworska, J. Chen, L. Pszczó kowski, P. Gawryś, J. Kosarzewski, Rotational spectroscopy and precise molecular structure of 1,2dichlorobenzene, J. Mol. Spectrosc. 374 (2020), 111380.
- [12] S.D. Sharma, S. Doraiswamy, Microwave spectrum, centrifugal distortion constants, and quadrupole coupling constants of 3-chloropyridine, J. Mol. Spectrosc. 57 (1975) 377–390.
- [13] Y. Sasada, M. Saitoh, S. Tobita, Microwave spectrum and nuclear quadrupole coupling of 3-bromothiophene, J. Mol. Spectrosc. 92 (1982) 363–374.
- [14] S. Doraiswamy, S.D. Sharma, Quadrupole coupling constants and centrifugal distortion constants of 3-bromopyridine from its microwave spectrum, J. Mol. Spectrosc. 88 (1981) 95–108.
- [15] J. Chen, C.D. Paulse, R.W. Davis, The microwave spectrum, electric dipole moment, and bromine nuclear quadrupole coupling constants of 2bromopyrimidine, J. Mol. Spectrosc. 145 (1991) 18 28.

- [16] P.M. Higgins, B.J. Esselman, M.A. Zdanovskaia, R.C. Woods, R.J. McMahon, Millimeter-wave spectroscopy of the chlorine isotopologues of chloropyrazine and twenty-two of their vibrationally excited states, J. Mol. Spectrosc. 364 (2019), 111179
- [17] B.J. Esselman, M.A. Zdanovskaia, R.C. Woods, R.J. McMahon, Millimeter-wave spectroscopy of the chlorine isotopologues of 2-chloropyridine and twenty-three of their vibrationally excited states, J. Mol. Spectrosc. 365 (2019), 111206.
- [18] B.A. McGuire, A.M. Burkhardt, S.V. Kalenskii, C.N. Shingledecker, A.J. Remijan, E. Herbst, M.C. McCarthy, Detection of the aromatic molecule benzonitrile (c-C₆H₅CN) in the interstellar medium, Science 359 (2018) 202–205.
- [19] B.A. McGuire, R.A. Loomis, A.M. Burkhardt, K.L.K. Lee, C.N. Shingledecker, S. B. Charnley, I.R. Cooke, M.A. Cordiner, E. Herbst, S. Kalenskii, M.A. Siebert, E. R. Willis, C. Xue, A.J. Remijan, M.C. McCarthy, Detection of two interstellar polycyclic aromatic hydrocarbons via spectral matched filtering, Science 371 (2021) 1265–1269.
- [20] M.C. McCarthy, K.L.K. Lee, R.A. Loomis, A.M. Burkhardt, C.N. Shingledecker, S. B. Charnley, M.A. Cordiner, E. Herbst, S. Kalenskii, E.R. Willis, C. Xue, A. J. Remijan, B.A. McGuire, Interstellar detection of the highly polar five-membered ring cyanocyclopentadiene, Nat. Astron. 5 (2021) 176 180.
- [21] J. Cernicharo, M. Agúndez, C. Cabezas, B. Tercero, N. Marcelino, J.R. Pardo, P. de Vicente, Pure hydrocarbon cycles in TMC-1: discovery of ethynyl cyclopropenylidene, cyclopentadiene, and indene, Astron. Astrophys. 649 (2021) 115
- [22] J. Cernicharo, M. Agúndez, R.I. Kaiser, C. Cabezas, B. Tercero, N. Marcelino, J. R. Pardo, P. de Vicente, Discovery of benzyne, o-C₆H₄, in TMC-1 with the QUIJOTE line survey, Astron. Astrophys. 652 (2021) 1.9.
- [23] E.C. Fayolle, K.I. Öberg, J.K. J rgensen, K. Altwegg, H. Calcutt, H.S.P. Müller, M. Rubin, M.H.D. van der Wiel, P. Bjerkeli, T.L. Bourke, A. Coutens, E.F. van Dishoeck, M.N. Drozdovskaya, R.T. Garrod, N.F.W. Ligterink, M.V. Persson, S. F. Wampfler, H. Balsiger, J.J. Berthelier, J. De Keyser, B. Fiethe, S.A. Fuselier, S. Gasc, T.I. Gombosi, T. Sémon, C.Y. Tzou, the ROSINA team, Protostellar and cometary detections of organohalogens, Nat. Astron. 1 (2017) 703 708.
- [24] S. Albert, K. Keppler, P. Lerch, M. Quack, A. Wokaun, Synchrotron-based highest resolution FTIR spectroscopy of chlorobenzene, J. Mol. Spectrosc. 315 (2015) 92, 101
- [25] D.H. Whiffen, Vibrational frequencies and thermodynamic properties of fluorochloro-, bromo-, and iodo-benzene, J. Chem. Soc. 1350 1356 (1956).
- [26] H.D. Bist, V.K. Sarin, A. Ojha, Y.S. Jain, The planar vibrations of chlorobenzene in the ground state from an analysis of 2699 Å electronic band system, Spectrochim. Acta. Part A 26 (1970) 841–847.
- [27] H.D. Bist, V.N. Sarin, A. Ojha, Y.S. Jain, The 2699 Å electronic band system of chlorobenzene the in-plane vibrational modes in the excited state, Appl. Spectrosc, 24 (1970) 292–294.
- [28] Y.S. Jain, H.D. Bist, The out-of-plane vibrational modes of chlorobenzene in its ground and first singlet excited states, J. Mol. Spectrosc. 47 (1973) 126–133.
- [29] M.A. Zdanovskaia, K. Belmont, N. Love, B.J. Esselman, R.C. Woods, R.J. McMahon, Millimeter-wave spectrum of 2-chloropyrimidine in the ground and nine low-lying vibrational states, Unpublished Work.
- [30] B.J. Esselman, R.C. Woods, R.J. McMahon, Millimeter-wave Spectrum of 3-chloropyridine, Unpublished Work.
- [31] B.J. Esselman, B.K. Amberger, J.D. Shutter, M.A. Daane, J.F. Stanton, R.C. Woods, R.J. McMahon, Rotational spectroscopy of pyridazine and its isotopologs from 235 360 GHz: equilibrium structure and vibrational satellites, J. Chem. Phys. 139 (2013), 224304.
- [32] B.K. Amberger, B.J. Esselman, J.F. Stanton, R.C. Woods, R.J. McMahon, Precise equilibrium structure determination of hydrazoic acid (HN₃) by millimeter-wave spectroscopy, J. Chem. Phys. 143 (2015), 104310.
- [33] M.A. Zdanovskaia, B.J. Esselman, H.S. Lau, D.M. Bates, R.C. Woods, R.J. McMahon, Z. Kisiel, The 103 360 GHz rotational spectrum of benzonitrile, the first interstellar benzene derivative detected by radioastronomy, J. Mol. Spectrosc. 351 (2018) 39 48.
- [34] K.N. Crabtree, M.-A. Martin-Drumel, G.G. Brown, S.A. Gaster, T.M. Hall, M. C. McCarthy, Microwave spectral taxonomy: a semi-automated combination of chirped-pulse and cavity Fourier-transform microwave spectroscopy, J. Chem. Phys. 144 (2016), 124201.
- [35] Z. Kisiel, L. Pszczó kowski, I.R. Medvedev, M. Winnewisser, F.C. De Lucia, E. Herbst, Rotational spectrum of trans trans diethyl ether in the ground and three excited vibrational states, J. Mol. Spectrosc. 233 (2005) 231 243.
- [36] Z. Kisiel, L. Pszczó kowski, B.J. Drouin, C.S. Brauer, S. Yu, J.C. Pearson, I. R. Medvedev, S. Fortman, C. Neese, Broadband rotational spectroscopy of

- acrylonitrile: vibrational energies from perturbations, J. Mol. Spectrosc. 280 (2012) 134 144.
- [37] H.M. Pickett, The fitting and prediction of vibration-rotation spectra with spin interactions, J. Mol. Spectrosc. 148 (1991) 371 377.
- [38] Z. Kisiel, Assignment and Analysis of Complex Rotational Spectra, in: J. Demaison, K. Sarka, E.A. Cohen (Eds.), Spectroscopy from Space, Springer, Netherlands, Dordrecht, 2001, pp. 91–106.
- [39] Z. Kisiel, PROSPE Programs for ROtational SPEctroscopy. http://info.ifpan.edu. pl/~kisiel/prospe.htm.
- [40] A.N. Owen, M.A. Zdanovskaia, B.J. Esselman, J.F. Stanton, R.C. Woods, R. J. McMahon, Semi-experimental equilibrium (r_e^{SE}) and theoretical structures of pyridazine (o-C₄H₄N₂), J. Phys. Chem. A 125 (2021) 7976 7987.
- [41] V.L. Orr, Y. Ichikawa, A.R. Patel, S.M. Kougias, K. Kobayashi, J.F. Stanton, B. J. Esselman, R.C. Woods, R.J. McMahon, Precise equilibrium structure determination of thiophene (c-C₄H₄S) by rotational spectroscopy structure of a five-membered heterocycle containing a third-row atom, J. Chem. Phys. 154 (2021), 244310.
- [42] B.J. Esselman, M.A. Zdanovskaia, A.N. Owen, J.F. Stanton, R.C. Woods, R. J. McMahon, Precise equilibrium structure of thiazole (c-C₃H₃NS) from twenty-four isotopologues, J. Chem. Phys. 155 (2021), 054302.
- [43] Z.N. Heim, B.K. Amberger, B.J. Esselman, J.F. Stanton, R.C. Woods, R.J. McMahon, Molecular structure determination: equilibrium structure of pyrimidine (m-C₄H₄N₂) from rotational spectroscopy (r_e^{SE}) and high-level *ab initio* calculation (r_e) agree within the uncertainty of experimental measurement, J. Chem. Phys. 152 (2020), 104303.
- [44] J. Demaison, L. Margulès, J.E. Boggs, Equilibrium structure and force field of NH₂, Phys. Chem. Chem. Phys. 5 (2003) 3359–3363.
- [45] V. Tyuterev, S. Tashkun, H. Seghir, High-order contact transformations: general algorithm, computer implementation, and triatomic tests, Proc. SPIE 5311 (2004) 164 175.
- [46] L. Margulès, R.A. Motiyenko, J. Demaison, Millimeterwave and submillimeterwave spectra of sulfur dioxide ³²C₁6O₁8O and ³²C₁8O₂, centrifugal distortion analysis and equilibrium structure, J. Quant. Spectrosc. Radiat. Transfer 253 (2020), 107153.
- [47] V. Tyuterev, S. Tashkun, M. Rey, A. Nikitin, High-order contact transformations of molecular Hamiltonians: general approach, fast computational algorithm and convergence of ro-vibrational polyad models, Mol. Phys. (2022) e2096140.
- [48] M.A. Zdanovskaia, P.R. Franke, B.J. Esselman, B.E. Billinghurst, J. Zhao, J. F. Stanton, R.C. Woods, R.J. McMahon, Vibrationally excited states of 1*H* and 2*H* 1,2,3-triazole isotopologues analyzed by millimeter-wave and high-resolution infrared spectroscopy with approximate state-specific quartic distortion constants, J. Chem. Phys. 158 (2023), 044301.
- [49] M.J. Frisch, G.W. Trucks, H.B. Schlegel, G.E. Scuseria, M.A. Robb, J.R. Cheeseman, G. Scalmani, V. Barone, G.A. Petersson, H. Nakatsuji, X. Li, M. Caricato, A.V. Marenich, J. Bloino, B.G. Janesko, R. Gomperts, B. Mennucci, H.P. Hratchian, J.V. Ortiz, A.F. Izmaylov, J.L. Sonnenberg, D. Williams-Young, F. Ding, F. Lipparini, F. Egidi, J. Goings, B. Peng, A. Petrone, T. Henderson, D. Ranasinghe, V.G. Zakrzewski, J. Gao, N. Rega, G. Zheng, W. Liang, M. Hada, M. Ehara, K. Toyota, R. Fukuda, J. Hasegawa, M. Ishida, T. Nakajima, Y. Honda, O. Kitao, H. Nakai, T. Vreven, K. Throssell, J.A. Montgomery, Jr., J.E. Peralta, F. Ogliaro, M.J. Bearpark, J.J. Heyd, E.N. Brothers, K.N. Kudin, V.N. Staroverov, T.A. Keith, R. Kobayashi, J. Normand, K. Raghavachari, A.P. Rendell, J.C. Burant, S.S. Iyengar, J. Tomasi, M. Cossi, J.M. Millam, M. Klene, C. Adamo, R. Cammi, J.W. Ochterski, R.L. Martin, K. Morokuma, O. Farkas, J.B. Foresman, D.J. Fox, Gaussian 16 rev C.01. Gaussian, Inc., Wallingford, CT, USA, 2016.
- [50] J.R. Schmidt, W.F. Polik, WebMO Enterprise, version 19.0; WebMO LLC: Madison, WI, USA, 2019, http://www.webmo.net (accessed August, 2019).
- [51] M.A. Zdanovskaia, B.J. Esselman, R.C. Woods, R.J. McMahon, The 130 370 GHz rotational spectrum of phenyl isocyanide (C₆H₅NC), J. Chem. Phys. 151 (2019), 024301.
- [52] P.M. Dorman, B.J. Esselman, J.E. Park, R.C. Woods, R.J. McMahon, Millimeter-wave spectrum of 4-cyanopyridine in its ground state and lowest-energy vibrationally excited states, 20 and 30, J. Mol. Spectrosc. 369 (2020), 111274.
- [53] P.M. Dorman, B.J. Esselman, R.C. Woods, R.J. McMahon, An analysis of the rotational ground state and lowest-energy vibrationally excited dyad of 3-cyanopyridine: low symmetry reveals rich complexity of perturbations, couplings, and interstate transitions, J. Mol. Spectrosc. 373 (2020), 111373.
- [54] V.L. Orr, B.J. Esselman, P.M. Dorman, B.K. Amberger, I.A. Guzei, R.C. Woods, R. J. McMahon, Millimeter-wave spectroscopy, X-ray crystal structure, and quantum chemical studies of diketene resolving ambiguities concerning the structure of the ketene dimer, J. Phys. Chem. A 120 (2016) 7753 7763.